Project THEMIS
Technical Report No. 19

MASS DISPERSION FROM AN INSTANTANEOUS LINE SOURCE IN A TURBULENT SHEAR FLOW

by
S. N. Putta
and
J. E. Cermak

Prepared under
Office of Naval Research
Contract No. N00014-68-A-0493-0001
Project No. NR 062-414/6-6-68 (Code 438)
U. S. Department of Defense
Washington, D.C.

Fluid Dynamics and Diffusion Laboratory
College of Engineering
Colorado State University
Fort Collins, Colorado

June 1971

CER71-72SNP-JEC1

ABSTRACT

MASS DISPERSION FROM AN INSTANTANEOUS LINE SOURCE IN A TURBULENT SHEAR FLOW

Dispersion of passive material released from an instantaneous line source in the constant stress region of a neutral atmosphere is investigated. Concentration fields within the cloud of dispersing material is represented by a three dimensional density function. This density function is divided into a marginal density function and a conditional longitudinal density function. The marginal density function gives the vertical spread of the material. This function has been derived from the semiempirical equation of dispersion, by using logarithmic velocity distribution for mean velocity and a linear variation for eddy diffusivity in the vertical direction. Longitudinal density function, which gives the longitudinal distribution of material within a given horizontal layer of the cloud, is constructed from the statistical properties of dispersion. Utilizing the Lagrangian similarity hypothesis for the concentration field, the semiempirical equation has been transformed into a similarity coordinate plane. Moment equations are derived from this equation using suitable boundary conditions. From these equations statistical properties are derived for mean, variance and skewness coefficients of the longitudinal density function. It is shown that the longitudinal density function can be well represented by the Gram-Charlier density simply by substituting the derived statistical properties. Ground level concentrations obtained by integration of this proposed density function agree qualitatively with observations in wind tunnels and field experiments.

ACKNOWLEDGMENT

This study was initiated by Deseret Test Center (Dugway Proving Ground) as an attempt to determine feasibility of wind tunnel modeling of meteorological processes controlling the diffusion from an instantaneous line source as an alternative to making extensive field measurements. Field data reported by MacCready et al and Smith et al were provided for comparative purposes. Initial funding for the wind tunnel study was provided by program 1T062111A128 through contract DAAB07-68-C-0423, which is currently monitored by the United States Army Electronics Command (ECOM) and administered by the United States Army Materiel Command (AMC). Funds for completion were provided by the Office of Naval Research - Contract No. N0014-68-A-0493-0001.

TABLE OF CONTENTS

TABLE OF CONTENTS - (Continued)

LIST OF FIGURES

LIST OF SYMBOLS

Symbol	Definition
A	Constant of integration.
a	Constant in horizontal variance σ_x^2 .
b	Batchelor constant.
b'	Monin-Pasquill constant.
C	Concentration in three dimensional diffusion.
c'	Fluctuating part of concentration.
$E_1(\eta)$	Exponential integral.
f	Conditional density function for the direction of mean flow.
F	Similarity density function.
h	Height of an elevated source.
K_M	Coefficient of molecular diffusion.
K_{Tij}	Coefficient of turbulent diffusion tensor.
$K(\alpha;z,t)$	Cumulant function.
$\kappa_n(z,t)$	Cumulants.
t	Time of flight of cloud.
V_i	Component of velocity in cartesian coordinates.
u_i'	Components of fluctuating velocity.
u',v',w'	Components of fluctuating velocity in longitudinal, lateral and vertical directions.
u_*	Shear velocity.
$\overline{x}(t)$	Center of mass of cloud.
$x_m(z,t)$	Mean of concentration distribution for the direction of mean flow.
x_i	Cartesian coordinates.

Symbol	Definition
x,y,z	Dimensions in cartesian coordinates (longitudinal, lateral and vertical).
W	Length of cloud at ground level.
$\overline{z}(t)$	Center of mass of cloud.
z_{max}	Maximum height of cloud.
z_o	Roughness coefficient.
α	Parameter in characteristic function.
$\beta=\frac{x-\overline{x}}{au_*t}$	Similarity coordinate in 'x' direction.
γ	Euler constant.
$\Gamma(a,\eta)$	Incomplete gamma function.
$\Gamma'(a,\eta)$, $\Gamma''(a,\eta)$, $\Gamma^n(a,\eta)$	Derivatives of incomplete gamma function.
$\theta_n(z,t)$	n^{th} moment of density function about the center of mass.
$\eta=z/\kappa u_*t$	Similarity coordinates in 'z' direction.
κ	Von Karman constant.
$\xi=\frac{x-\mu}{au_*t}$	Normalized coordinate in 'x' direction.
$\sigma_x,\sigma_y,\sigma_z$	Standard deviation of density function for x,y,z directions.
$\mu(z,t)$	Mean of longitudinal density function.
λ_3	Skewness coefficient.
λ_4	Flatness factor
ψ	Nondimensional mean of the longitudinal density function.

Symbol	Definition
$\chi(x,z,t)$	Concentration in two dimensional diffusion.
$\chi_*(z,t)$	Marginal density function.

CHAPTER I

INTRODUCTION

Among a wide variety of problems concerning turbulent diffusion, studies of atmospheric diffusion occupy a central place in the literature. In recent studies, diffusion in the surface layer of the atmosphere has been of greatest interest, as the air in this layer is directly related to the life and vital activity of man. Examinations of air quality indicate an increased demand for pollution studies. It is important to understand the dynamics of the atmosphere in order to regulate or relocate the sources of pollution, so that the contaminants may be dispersed effectively. Fortunately, the atmosphere is turbulent most of the time, which helps in dispersing the matter more rapidly. However, in certain geographical locations where atmospheric motions are inhibited by natural restrictions or artificial creations, it becomes essential to position the sources and regulate the releases, so that the concentration level of contaminants are kept within permissible limits. In the past two decades considerable progress has been made towards the understanding of dispersion processes in turbulent shear flows. Applications of these studies to numerous pollution control problems, mechanism of pesticide and insecticide spreads, city and industrial plannings are in progress.

Pollutants from industrial smokestacks are continuous point sources. In the past two decades considerable work has been done, to give reliable estimates of concentration levels of pollution in the vicinity of a source, as an aid to planning industrial stacks. Important results are: the maximum ground level concentration is inversely proportional to the square of the height of the stack; and, the location of maximum concentration from the stack center is directly proportional to the height of the stack. Various formulae are available for plume rise calculations, depending on the exit velocity and buoyancy level of the gases. A comprehensive formula for dispersion estimates has been published by Turner [1969].

Radioactive effluents from atomic tests and volcanic ashes, gases from aircraft and automobiles, pollen from plants and the spread of agricultural insecticides and pesticides belong to a class of instantaneous sources. There are hardly any formula available from which to make reliable estimates about the dispersion of effluents from these kinds of sources. Some equations were suggested by Sutton [1932] for ground level concentrations due to instantaneous sources. These equations contain dispersion parameters such as σ_x , σ_y and σ_z , for which there are no analytical estimates available. Frenkiel and Katz [1953] conducted experiments on dispersion of smoke puffs in the surface layer of atmosphere. By analyzing the visible diameters of dispersing smoke puffs, they concluded that the dispersion parameters 'σ' are proportional to the square of time of dispersion.

Analytical studies of dispersion of instantaneous sources in the atmosphere have been published by Monin [1959], Saffman [1963] and Chatwin [1968]. Monin derived a marginal density function which determines the vertical spread of material released from an instantaneous point source. Saffman derived solutions for the first two statistical moments of density function for an instantaneous point source, by using linear velocity distribution for the surface shear flow. Chatwin derived solutions for the zero, first and second moments for the concentration distribution at ground level. Density function for the spatial distributions of concentration within the smoke puffs is not available for the sources released in the surface layer of atmosphere. A complete knowledge of the statistical properties of concentration distribution within the smoke puffs is essential to specify a function for a two or three dimensional density and to determine the probable shapes of smoke puffs.

It is the purpose of this present work to determine the statistical properties of the dispersion of contaminants released from an instantaneous line source and to specify a realistic probability density function for the spatial distribution of concentrations within the smoke puff. A probable shape of smoke puff will be presented for a source released at ground level. However, for sources released at a height 'h' above the ground, the results will still be valid for time 't' greater than t_1 , where t_1 is of the order of h/u_* . The formulae developed in this theory can be utilized in estimating the ground level exposures in farm fields where insecticides and pesticides are spread by aircraft.

CHAPTER II

THEORETICAL BACKGROUND

Problems of turbulent diffusion are complex and many sided. They have been subjected to theoretical and experimental investigation in the past few decades. Studies are mainly oriented towards the prediction of average concentration distribution of contaminants, released from various kinds of sources. As mentioned earlier, various formula are available for the dispersion of contaminants from continuous sources. But there are hardly any formula available for the estimation of concentration levels due to instantaneous sources. In this chapter a review of pertinent theories is presented. Eulerian equations of dispersion are derived. Lagrangian similarity theory is discussed. Governing equations for dispersion of contaminants from instantaneous sources are formulated, by coupling the Lagrangian similarity theory with Eulerian equations.

2.1. Description of Turbulent Diffusion

When an admixture is introduced into a turbulent flow, it is rapidly spread in the volume occupied by the fluid as a result of transfer mechanism of the flow. This phenomenon called turbulent diffusion is an important characteristic of turbulent flows. The admixture can be in the form of liquid, gaseous additive or in the form of large numbers of fine particles.

In each individual realization of turbulent flow, the field of concentration $C(x_i,t)$ in regions which do not contain sources or sinks, satisfies the equation of molecular diffusion

$$\frac{\partial C}{\partial t} + \frac{\partial U_i C}{\partial x_i} = \nabla \cdot K_M \nabla C \quad . \tag{2.1}$$

For a passive admixture the velocity field does not depend on the concentration field. Hence the equation remains linear with regard to concentration. More often the boundary conditions are also linear with respect to 'C'. They are of the form

$$K_M \frac{\partial C}{\partial n} + \phi C = f(t) \tag{2.2}$$

where 'n' is normal to the boundary and ϕ is a constant. In the case of solid walls which bound the flow, the boundary conditions are homogeneous, that is $f(t) = 0$

$$
\begin{aligned}
K_M \frac{\partial C}{\partial n} + \phi C &= 0 && \text{at solid wall} \\
\phi &= \infty && \text{for completely absorbing boundary} \\
\phi &= 0 && \text{completely reflecting boundary} \\
0 < \phi &< \infty && \text{partial absorbing boundary}
\end{aligned}
\tag{2.3}
$$

For the flow which is unlimited in any direction, the boundary condition becomes

$$C \to 0 \quad \text{as} \quad x_i \to \infty$$

Boundary conditions of the type $f(t) \neq 0$, correspond to continuously active sources. We will limit out discussion to homogeneous boundary conditions only.

2.2. Eulerian Equation of Turbulent Diffusion

Determination of the average concentration field $\overline{C}(x_i,t)$ is the most important and desirable problem of turbulent diffusion. The governing equation for such a field is obtained by averaging all the terms in equation (2.1) using the following perturbation theory.

$$\frac{\partial C}{\partial t} + \frac{\partial U_i C}{\partial x_i} = \nabla \cdot K_M \nabla \overline{C}$$

where
$$C = \overline{C} + c' \qquad \overline{c'} = 0$$

$$U_i = \overline{U}_i + u_i' \qquad \overline{u_i'} = 0 \ .$$

Using the above averaging process, we obtain

$$\frac{\partial \overline{C}}{\partial t} + \frac{\partial \overline{U_i C}}{\partial x_i} = - \frac{\partial \overline{u_i' \, c'}}{\partial x_i} + \nabla \cdot K_M \nabla \overline{C} \tag{2.4}$$

$\overline{c'u_i'}$ are not known <u>a priori</u>, but they may be related to a gradient of mean concentration by the well known gradient transfer relation as suggested by G. I. Taylor [1915] and Schmidt [1917]. The eddy transfer of material across a plane is represented as a product of gradient of material and the eddy diffusivity K_T

$$-\overline{c'u_i'} = K_{T_{ij}} \frac{\partial \overline{C}}{\partial x_j} \ . \tag{2.5}$$

Now equation (2.4) becomes

$$\frac{\partial \overline{C}}{\partial t} + \frac{\partial \overline{U_i C}}{\partial x_i} = \frac{\partial}{\partial x_i} K_{T_{ij}} \frac{\partial \overline{C}}{\partial x_j} + \nabla \cdot K_M \nabla \overline{C} \ . \tag{2.6}$$

The processes of molecular and turbulent diffusion are independent and therefore additive [Mickelson 1960]

$$K_{ij}\,(x_i) = K_{T_{ij}} + K_M \tag{2.7}$$

K_{ij} is a diffusion tensor which can be replaced by scalar K_i , by taking axes of the coordinate system as the principle axes of the tensor.

$$\text{Then}\quad K_{ij} = 0 \quad \text{for} \quad i \neq j$$
$$= K_i \quad \text{for} \quad i = j$$

Then the dispersion equation becomes (eliminating the overbars for the sake of expedience):

$$\frac{\partial C}{\partial t} + \frac{\partial U_i C}{\partial x_i} = \frac{\partial}{\partial x_i} \left(K_i \frac{\partial C}{\partial x_i}\right) \tag{2.8}$$

Integrating the equation (2.8) for the lateral direction 'y' , a dispersion equation for infinite crosswind line source is obtained.

Writing $\int_{-\infty}^{\infty} C\,dy = \chi(x,z,t)$ we obtain

$$\frac{\partial \chi}{\partial t} + \frac{\partial U_1 \chi}{\partial x} + \frac{\partial U_3 \chi}{\partial z} = \frac{\partial}{\partial x} \left(K_x \frac{\partial \chi}{\partial x}\right) + \frac{\partial}{\partial z} \left(K_z \frac{\partial \chi}{\partial z}\right) \;. \tag{2.9}$$

In the absence of vertical velocity 'U_3' , and horizontal velocity gradient $\frac{\partial U_1}{\partial x}$ (under the adiabatic conditions of the atmosphere in the surface layer), we can write the dispersion equation as

$$\frac{\partial \chi}{\partial t} + U_1 \frac{\partial \chi}{\partial x} = \frac{\partial}{\partial x} \left(K_x \frac{\partial \chi}{\partial x}\right) + \frac{\partial}{\partial z} \left(K_z \frac{\partial \chi}{\partial z}\right) \tag{2.10}$$

2.3. Lagrangian Characteristics of Turbulent Diffusion in the Boundary Layer

Consider a particle released in turbulent flow at a point $(x,y,z) = (0,0,h)$ respectively, at time $t = t_o$, where x is the direction of mean flow, y is the crosswind direction and z is vertical direction. Let $x(t)$, $y(t)$, $z(t)$ be the coordinates of this particle at time t_o+t , and $U(t)$, $V(t)$, $W(t)$ be the components of velocity $\vec{V}(t)$ of the particle in the x,y,z directions. As time increases the particle rises significantly and the horizontal velocity $U(t)$ increases strongly. Hence, the random function $\vec{V}(t)$ is not stationary. Generally speaking, there is no basis for considering that the function $\vec{V}(t)$ may be transformed into stationary function with the help of a simple transition to new scales of length and time. In addition to the parameters, length 'ℓ' and time 't' , Lagrangian characteristics of turbulence depend upon a few external parameters which determine the turbulent condition. As stated by Monin and Yaglom [1966], it is natural to assume that these parameters enter into the expression for Eulerian statistical characteristics. Hence, some information can be obtained by coupling the Lagrangian equations of diffusion with the Eulerian equations. One possible way of coupling these equations is by substituting the results of Lagrangian similarity theory into the Eulerian equations (2.8). The author feels that this is a more convenient way of obtaining any statistical information about turbulent diffusion of instantaneous sources. Such an evaluation of statistical properties is essential for making any estimates about dispersion of mass from instantaneous sources.

In the next section, Lagrangian similarity theory is presented Results of this theory will be utilized to derive statistical properties of dispersion, from the Eulerian equations.

2.4. Similarity Theories on Turbulent Diffusion

The concept of similarity of various statistical functions describing turbulent velocity fluctuations has proved to be exceedingly useful in the theory of turbulent jets, wakes and mixing layers. Such an observation led the scientists, particularly A. S. Monin and G. K. Batchelor, to extend similarity concept to diffusion processes in turbulent flows. They noted that the motion of fluid particles in the constant stress region of the turbulent boundary layer have certain similarity properties, which can be used to predict some features of turbulent diffusion. Monin [1959] demonstrated that turbulent diffusion in a horizontally homogeneous, stationary, surface layer of air, obeys the similarity theory in which, the values of shear velocity 'u_*' and the stability length 'L', are the only scales of velocity and length. For neutral flows where the scale 'L' does not exist, Batchelor [1959] proposed the following similarity hypothesis, which is Lagrangian in nature. Statistical properties of the velocity of a marked fluid particle depend only on u_* and the time of travel 't'. Assuming this hypothesis to be valid, he obtained the following results. Center of mass of a cloud of diffusing particles $(\overline{x},\overline{z})$ satisfies the equation

$$\frac{d\overline{z}}{dt} = bu_*, \quad \overline{z} = bu_*t$$

$$\frac{d\overline{x}}{dt} = U(c\overline{z}) \tag{2.11}$$

where b and c are universal constants. With these results in mind he proposed a probability density function for positions (x,y,z) of dispersing particles (released at or near ground level at time t = 0) as

$$C(x,y,z|t) = \frac{1}{(bu_*t)^3} f\left(\frac{x-\bar{x}}{bu_*t}, \frac{y}{bu_*t}, \frac{z}{bu_*t}\right) .$$

For a two dimensional situation the density function becomes,

$$\chi(x,z|t) = \int_{\infty}^{\infty} c(x,y,z|t)\, dy = \frac{1}{(bu_*t)^2} F\left(\frac{x-\bar{x}}{bu_*t}, \frac{z}{bu_*t}\right) .$$

The forms of density functions 'f' and F are not known.

During the last ten years, considerable work has been done on the validity and application of similarity theory to turbulent diffusion in the atmospheric surface layer. Batchelor [1964] and Ellison [1959] applied the similarity hypothesis for adiabatic flows in the surface layer and derived equations for the relative ground level concentrations downwind of continuous point and crosswind line sources. Gifford [1962] derived expressions for some statistical properties for diffusion in stratified flows. Cermak [1963] has derived formulae for concentration decay rates and for plume width of continuous sources in both stratified and neutral flows. He compared his results with experimental data from Porton [1962], Project Prairie grass [1957] and with wind tunnel data at Colorado State University (reported by Malhotra [1962], Davar [1961] and Poreh [1962]). Saffman [1962] derived expressions for statistical properties of longitudinal density function by using linear velocity profile in the surface layer. Panofsky and

Prasad [1965] analyzed the results of similarity theories on statistical properties of turbulent velocities with the observations that the lateral velocity fluctuations do not support similarity theory in the case of stratified flows. However, no objection was raised against similarity theory in the case of neutral flows. Pasquill [1966] and Klugg [1968] compared the vertical standard deviation σ_z of concentration from diffusion experiments with the results of similarity theory. Iordanov [1966] obtained equations for vertical transfer of material for an instantaneous crosswind line source, by assuming a function for eddy diffusivity K_z that contains two expressions for two regions of height. Chatwin [1968] derived expressions for statistical properties of dispersing material released from an instantaneous line source. He solved for the first and second moments of longitudinal density function by assuming Lagrangian similarity for the density function.

In all these published works, there appears very little progress towards the determination of density functions for 'C' and χ. It is the purpose of the present work to specify the density function for 'χ', for dispersion of material in the surface layer of atmosphere. Lagrangian similarity will be assumed for the solution of Eulerian equations. Various statistical properties will be derived from the resulting equations of motion. With the knowledge of these properties, a probable density function will be specified. Shape of the diffusing cloud will be presented in suitable figures.

CHAPTER III

THEORETICAL ANALYSIS

In this chapter statistical properties of a dispersing cloud are obtained for a source released at ground level. Eulerian dispersion equation (2.10) represented the mechanism of the dispersing field. Batchelor's constants 'b' and 'c' are derived, using logarithmic and power laws for the velocity profile, and conjugate laws for the eddy diffusivity. Utilizing Batchelor's [1964] Lagrangian similarity hypothesis, the unsteady state dispersion equation is reduced to a steady state. This steady state equation has been utilized to determine the moments of the density function. These central moments, namely, 0th, 1st, 2nd and 3rd moments are used in specifying the density function for the concentration field within the dispersing cloud.

3.1. Density Function

In homogeneous turbulent flow, Batchelor [1958] has shown that the eddy velocities u', v' and w' are distributed according to Guassian law. For small dispersion times, since the particle trajectories coincide with the instantaneous wind, any passive contaminant released instantaneously into the flow is also distributed Gaussian. In the case of shear flow, distribution of contaminants released at the wall or near the wall may not be Gaussian. Velocity gradient present in the flow might interact with the turbulent intensity and introduce considerable skewness into the density function. In such cases it becomes necessary to evaluate higher order statistical moments, in order to specify a density function for a dispersing cloud of material released instantaneously in a turbulent shear flow.

For instantaneously released cross wind line source as shown in Fig. 1, the dispersing field of concentrations can be represented by a three dimensional density function as

$$\chi(x,z,t) = f(x|z,t)\ \chi_*(z,t)$$

where

$$\chi_*(z,t) = \int_{-\infty}^{\infty} \chi(x,z,t)\ dx \tag{3.1}$$

is a marginal density function and $f(x|z,t)$ is a conditional density function for the direction of mean flow, given z and t. These density functions satisfy the following relation for mass conservation.

$$\int_{0}^{\infty}\int_{\infty}^{\infty} \chi(x,z,t)\ dx\ dz = \int_{0}^{\infty}\int_{-\infty}^{\infty} f(x|z,t)\ \chi_*(z,t)\ dx\ dz$$

$$= \int_{0}^{\infty} \chi_*(z,t)\ dz = 1.0 \quad . \tag{3.2}$$

These density functions are now in a convenient form to determine their functional forms by using the dynamic equations of turbulent dispersion.

3.2. Density Function for the Direction of Mean Flow

Consider the Fourier transform of $f(x|z,t)$ given by

$$\phi\ (\alpha;z,t) = \int_{-\infty}^{\infty} e^{i\alpha x}\ f(x|z,t)\ dx = \overline{e^{i\alpha x}}\ (z,t) \quad . \tag{3.3}$$

Its inverse transform gives

$$f(x|z,t) = \frac{1}{2\pi} \int_{-\infty}^{\infty} e^{-i\alpha x}\ \phi(\alpha,z,t)\ d\alpha \quad . \tag{3.4}$$

Derivatives of $\phi(\alpha;z,t)$ at the origin $\alpha = 0$ are proportional to the moments. So the moments determine the series expansion of $\phi(\alpha;z,t)$, hence the density function $f(x|z,t)$.

$$\frac{\partial^n}{\partial(i\alpha)^n}\phi(\alpha;z,t)\Big|_{\alpha=0} = \overline{x^n}(z,t) = \mu_n(z,t) \quad n = 1,\ldots n$$

Taylor's expansion for $\phi(\alpha;z,t)$ gives

$$\phi(\alpha;z,t) = 1 + \frac{\mu_1(z,t)}{1!}(i\alpha) + \frac{\mu_2(z,t)}{2!}(i\alpha)^2 + \frac{\mu_3(z,t)}{3!}(i\alpha)^3 + \ldots$$

Consider now the cumulant function for convenience

$$K(\alpha;z,t) = \ell n\ \phi(\alpha;z,t)$$

Taylor's expansion for $K_n(\alpha\ ;z,t)$ gives

$$K(\alpha;z,t) = \frac{k_1(z,t)}{1!}(i\alpha) + \frac{k_2(z,t)}{2!}(i\alpha)^2 + \ldots$$

where $k_n(z,t) = \dfrac{\partial^n}{\partial(i\alpha)^n}\ell n\ \phi(\alpha;z,t)\Big|_{\alpha=0}$ are cumulants.

It can be shown that moments of the density function can be expressed by cumulants such as:

$$\mu_1(z,t) = \frac{\partial\phi(\alpha;z,t)}{\partial(i\alpha)}\Big|_{\alpha=0} = \frac{\partial}{\partial(i\alpha)}\exp\ [\ell n\ \phi(\alpha;z,t)\Big|_{\alpha=0} = k_1(z,t)$$

$$\mu_2(z,t) = \frac{\partial^2\phi(\alpha;z,t)}{\partial(i\alpha)^2}\Big|_{\alpha=0} = k_1^2\ (z,t) + k_2(z,t)$$

$$\mu_3(z,t) = \frac{\partial^3\phi(\alpha;z,t)}{\partial(i\alpha)^4}\Big|_{\alpha=0} = k_3 + 2k_2\ k_1 + k_1^3$$

Similarly, $\mu_4 = k_4 + 4\,k_1\,k_3 + 3k_2^2 + 6k_1^2\,k_2 + k_1^4$ (3.5)

$\vdots$

The coefficient of skewness and kurtosis can now be defined as

$$\lambda_3 = k_3/k_2^{3/2} \quad \text{and} \quad \lambda_4 = k_4/k_2^2 \quad .$$

Now the integral for the density function (3.8) becomes

$$f(x|z,t) = \frac{1}{2\pi}\int_{\infty}^{\infty} e^{-i\alpha x}\,\phi(\alpha;z,t)d\alpha$$

$$= \frac{1}{2\pi}\int_{-\infty}^{\infty} \exp\,[K(\alpha;z,t) - i\alpha x]d\alpha$$

$$= \frac{1}{2\pi}\int \exp\,[(k_1-x)i\alpha + \frac{1}{2}k_2(i\alpha)^2 + \frac{1}{6}k_3(i\alpha)^3 + \frac{1}{24}k_4\,(i\alpha)^4 \ldots]d\alpha$$

Substituting for $\alpha = s/k_2^{\frac{1}{2}}$ and $(x-k_1) = \xi\,k_2^{\frac{1}{2}}$, it can be shown that

$$f(x|z,t) = \frac{1}{2\pi k_2^{\frac{1}{2}}}\int_{-\infty}^{\infty} \mathrm{Exp}\,[-\frac{1}{2}(s^2 + 2i\xi s) + \frac{1}{6}\lambda_3\,(is)^3 + \frac{1}{24}\lambda_4(is)^4$$

$$+ \ldots\ldots.]ds.$$

Expanding the second group under the exponent it can be shown that

$$f(x|z,t) = \frac{1}{2\pi k_2^{\frac{1}{2}}}\int_{-\infty}^{\infty} \mathrm{Exp}\,[-\frac{1}{2}(s^2 + 2i\xi s)][1 + \frac{1}{6}\lambda_3\,(is)^3 + \frac{1}{24}\lambda_4\,(is)^4$$

$$+ \frac{1}{72}\lambda_3^2\,(is)^6 + \frac{\lambda_4{}^2}{1152}(is)^8 + \frac{\lambda_3\lambda_4}{144}(is)^7 + \ldots.]ds \quad .$$

Using the identity

$$(\frac{1}{2\pi})^{\frac{1}{2}}\int_{-\infty}^{\infty} \mathrm{Exp}\,[-\frac{1}{2}(s^2 + 2i\xi s)](is)^n\,ds = \frac{(-1)^n}{(2\pi)^{\frac{1}{2}}}\frac{\partial^n}{\partial\xi^n}\int_{-\infty}^{\infty} \mathrm{Exp}\,(-\frac{1}{2}(s^2 + 2i\xi s)ds$$

$$= (-1)^n \frac{d^n}{d\xi^n} e^{-\xi^2/2} = e^{-\xi^2/2} H_n(\xi)$$

where

$$H_n(\xi) = \xi^n - \frac{n(n-1)}{1!} \frac{\xi^{n-2}}{2} + \frac{n(n-1)(n-2)(n-3)}{2!} \frac{\xi^{n-4}}{2^2} - \ldots \tag{3.6}$$

are the Hermite polynomials of degree 'n' , the density function 'f' can be written as

$$f(x|z,t) = (2\pi k_2)^{-\frac{1}{2}}\left(1 + \frac{1}{6}\lambda_3 H_3 + \frac{1}{24}\lambda_4 H_4 + \frac{1}{72}\lambda_3^2 H_6 + \frac{1}{1152}\lambda_4^2 H_8 + \frac{1}{144}\lambda_3\lambda_4 H_7 + \ldots\ldots\right) \operatorname{Exp}(-\xi^2/2) \tag{3.7}$$

One finds here that $f(x|z,t)$ will be a normal density function when $\lambda_3 = \lambda_4 = 0$. Different values of λ_3 and λ_4 give different forms to the density function.

Hermite polynomial $H_3 = (\xi^3 - 3\xi)$ introduces skewness into the density function by shifting the mass from one side to the other according to the sign of the skewness coefficient λ_3 .

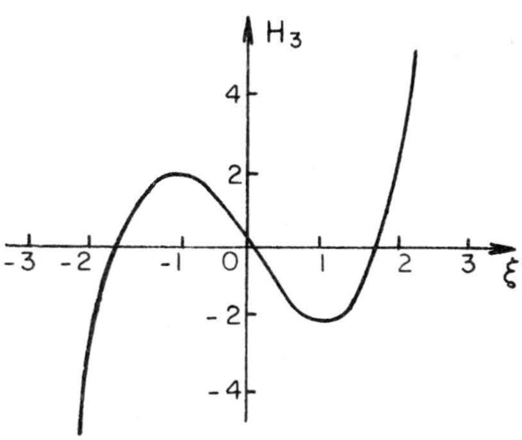

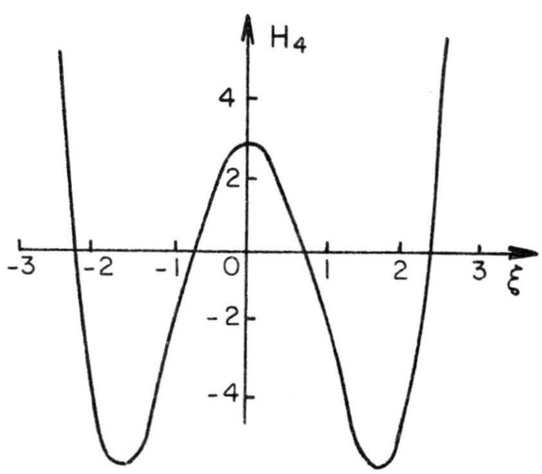

Hermite polynomial $H_4 = \xi^4 - 6\xi^2 + 3$ increases or reduces the peak of the density function depending on the sign of the flatness factor λ_4.

Hence, this type of density function is capable of handling any distortions in a realistic distribution of concentration field within a dispersing cloud, by having appropriate values for λ_3 and λ_4. The values of k_2, λ_3 and λ_4 are determined by the cumulants. These cumulants which can be obtained from the equations of dispersion, will be discussed in section 3.5.

3.3. Marginal Density Function $X_*(z,y)$

A differential equation for instantaneous cross wind line source is obtained by integrating the dispersion equation (2.8) for the lateral direction. In the absence of mean vertical velocity and horizontal velocity gradient $(\partial U_1/\partial x)$, such an equation has been shown in (2.10) as

$$\frac{\partial \chi}{\partial t} + U_1 \frac{\partial \chi}{\partial x} = \frac{\partial}{\partial x} (K_x \frac{\partial \chi}{\partial x}) + \frac{\partial}{\partial z} (K_z \frac{\partial \chi}{\partial z}) \tag{3.8}$$

Integration of this equation for the direction of 'x' yields a differential equation for χ_* as

$$\frac{\partial \chi_*}{\partial t} + \int_{-\infty}^{\infty} U_1 \frac{\partial \chi}{\partial x} \, dx = \int_{-\infty}^{\infty} \frac{\partial}{\partial x} (K_x \frac{\partial \chi}{\partial x}) \, dx + \int_{-\infty}^{\infty} \frac{\partial}{\partial z} (K_z \frac{\partial \chi}{\partial z}) \, dx$$

Using the boundary condition

$$K_x \frac{\partial \chi}{\partial x} \to 0 \quad \text{as} \quad x \to \pm \infty , \tag{3.9a}$$

it can be shown that

$$\frac{\partial \chi_*}{\partial t} + \int_{-\infty}^{\infty} U_1 \quad \partial \chi = \int_{-\infty}^{\infty} \frac{\partial}{\partial z} (K_z \frac{\partial \chi}{\partial z}) \, dx. \tag{3.9}$$

Here the functional forms for U_1 and K_z should be obtained from the characteristics of the representing flow field. Under adiabatic conditions, in the surface of the atmosphere there is enough support for the mean velocity distribution, that

$$\frac{U_1}{u_*} = \frac{1}{\kappa} \ell n \frac{z}{z_o} \tag{3.10}$$

when mass and momentum transfers are identically equal (Reynold's analogy; when the stress in the surface layer is constant it can be shown that

$$K_z = \kappa u_* z \quad . \tag{3.11}$$

Substituting (3.10) and (3.11) for U_1 and K_z , respectively, into (3.9) and performing the integration using the following boundary conditions

$$\begin{aligned} &\chi \to 0 \quad \text{as} \quad z \to \infty \\ &K_z \frac{\partial \chi}{\partial z} \to 0 \quad \text{as} \quad z \to 0 \end{aligned} \tag{3.12}$$

it can be shown that

$$\frac{\partial \chi_*}{\partial t} = \frac{\partial}{\partial z} [\kappa u_* z \frac{\partial \chi_*}{\partial z}] \tag{3.12a}$$

and the marginal density function as

$$\chi_*(z,t) = \frac{1}{\kappa u_* t} \exp(-z/\kappa u_* t) \quad . \tag{3.13}$$

Now the density function for the dispersion of contaminants from an instantaneous line source can be written as

$$\chi(x,z,t) = f(x|z,t) \quad \chi_*(z,t)$$

$$= \frac{1}{(2\pi k_2)^{\frac{1}{2}}} \left(1 + \frac{1}{6}\lambda_3 H_3 + \frac{1}{24}\lambda_4 H_4 + \frac{1}{72}\lambda_3^2 H_6 + \frac{1}{1152}\lambda_4^2 H_8 + \ldots\right) \exp\left(\frac{-\xi^2}{2} - \frac{z}{\kappa u_* t}\right) \tag{3.14}$$

The process of determining the first few moments of the density function 'f' and to obtain the parameters μ_1 , σ and λ_3 , is dealt with in the following sections.

3.4. Center of Mass of the Cloud-Determination of Batchelor's Constants 'b' and 'c'

Center of mass of the cloud is defined as

$$\bar{z} = \int_{-\infty}^{\infty} \int_{0}^{\infty} z \; \chi \; dz \; dx \quad \text{and} \quad \bar{x} = \int_{0}^{\infty} \int_{-\infty}^{\infty} x \; \chi \; dx \; dz \tag{3.14}$$

Multiplying the equation (3.8) by 'z' and performing the integration as in (3.14) it can be shown that

$$\frac{\partial \bar{z}}{\partial t} + \frac{u_*}{\kappa} \int_0^{\infty} z \; \ln \frac{z}{z_0} \left(\int_{-\infty}^{\infty} \frac{\partial \chi}{\partial x} dx \right) dz = \int_0^{\infty} z \frac{\partial}{\partial z} \left[\kappa u_* z \frac{\partial}{\partial z} \left(\int_{-\infty}^{\infty} \chi dx \right)\right] dz \; . \tag{3.15}$$

The second integral on the left hand side vanishes as 'χ' is zero at either of the limits of integration. Performing the integration on the right hand side of (3.15) using the boundary conditions (3.12) and the relation (3.13), it can be shown that

$$\frac{d\bar{z}}{dt} = - \int_0^{\infty} \kappa u_* z \frac{\partial \chi_*}{\partial z} dz = \int_0^{\infty} \kappa u_* \chi_* \; dz = \kappa u_*$$

and

$$\bar{z} = \kappa u_* t \tag{3.16}$$

comparing (3.16) with Batchelor's relation for $\bar{z}$ in (2.11) it can be shown that $b = \kappa$. The average vertical velocity is a constant in spite of the fact that the average vertical Euler velocity is zero at all points in the flow. This is due to the fact that the particle is free to rise but is prevented from a downward motion by the wall. Center of mass of the cloud rises linearly with time as predicted by G.K. Batchelor. The above results are obtained by Ellison [1957], Chatwin [1968] and Chaudhry [1969], etc.

<u>Comment</u> - By the use of power law relation for the mean velocity and conjugate law for the vertical eddy diffusivity, namely, $\bar{u} \propto z^{\alpha}$ and $K_z \propto z^{(1-\alpha)}$ in eq. (3.8) the following results are obtained.

$$\frac{d\bar{z}}{dt} \propto t^{-\frac{\alpha}{1+\alpha}} , \quad \bar{z} \propto t^{\frac{1}{1+\alpha}}$$

$$\overline{z^2} \propto t^{\frac{2}{1+\alpha}} \quad . \tag{3.17}$$

It shows that the rate of rise of center of mass of the cloud decreases with time for $\alpha > 0$.

Consider the dispersion equation (3.8). For long times after release. Monin [1966] and Saffman [1962] have shown that the longitudinal diffusion term $(\frac{\partial}{\partial x} K_x \frac{\partial \chi}{\partial x})$ contributes very little to the horizontal scattering compared to that caused by the interaction of vertical gradient of mean velocity with the vertical turbulence transfer. Hence, when this term is neglected equation (3.8) will be in a convenient form for determining the statistical properties of the density function.

$$\frac{\partial \chi}{\partial t} + (\frac{u_*}{\kappa} \ell n \frac{z}{z_o}) \frac{\partial \chi}{\partial x} = \frac{\partial}{\partial z} (\kappa u_* z \frac{\partial \chi}{\partial z}) \quad . \tag{3.18}$$

Multiplying (3.8) by 'x' and performing the integrations in space as in (3.14), a differential equation for $\bar{x}$ is obtained:

$$\frac{d\bar{x}}{dt} + \frac{u_*}{\kappa} \int_0^\infty \ln \frac{z}{z_o} \left(\int_{-\infty}^\infty x \frac{\partial \chi}{\partial x} dx \right) dz = \int_0^\infty \frac{\partial}{\partial z} \left(\kappa u_* z \frac{\partial}{\partial z} \int_{-\infty}^\infty x \frac{\partial \chi}{\partial x} dx \right) dz$$

Using boundary conditions (3.12), it can be shown that the integral on the right hand side is zero. Also it can be shown using boundary condition (3.9a)

$$\frac{d\bar{x}}{dt} = \frac{u_*}{\kappa} \int_0^\infty \ln \frac{z}{z_o} \left(\int_{-\infty}^\infty \chi dx \right) dz$$

$$= \frac{u_*}{\kappa} \int_0^\infty \ln \frac{z}{z_o} \quad \chi_* \, dz \qquad .$$

Substituting (3.13) for χ_* it can be shown that

$$\frac{d\bar{x}}{dt} = \frac{u_*}{\kappa} \int_0^\infty \left(\ln \frac{z}{z_o}\right) \frac{1}{\kappa u_* t} \exp\left(-z/\kappa u_* t\right) dz$$

$$= \frac{u_*}{\kappa} \left[\int_0^\infty \ln \frac{z}{\kappa u_* t} \exp\left(-z/\kappa u_* t\right) \frac{dz}{\kappa u_* t} - \ln \frac{z_o}{\kappa u_* t} \int_0^\infty \exp\left(\frac{-z}{\kappa u_* t}\right) \frac{dz}{\kappa u_* t} \right]$$

$$= \frac{u_*}{\kappa} \left[-\gamma + \ln \frac{\kappa u_* t}{z_o}\right] = \frac{u_*}{\kappa} \ln \frac{\kappa u_* t}{z_o e^\gamma}$$

where γ = Euler constant $\simeq 0.57721$

and

$$\bar{x} = \frac{u_* t}{\kappa} \left[\ln \left(\frac{\kappa u_* t}{z_o e^\gamma}\right) - 1\right] \quad \text{for} \quad t > \frac{4 z_o}{u_*} \tag{3.20}$$

Batchelor's Constant 'c' - Batchelor [1964] showed the following for the speed of the center of mass of the cloud in the directing mean flow:

$$\frac{d\bar{x}}{dt} = U(c\bar{z}) \qquad .$$

Comparing the result of Equation (3.19) and (3.10), it can be shown that

$$c = e^{-\gamma} = 0.5615 \tag{3.21}$$

The above results also are obtained by Chatwin [1968].

Comment - By the use of power law relation for the mean velocity and conjugate law for the vertical eddy diffusivity in Eq. (3.8), Batchelor's constant 'c' can be shown equal to

$$c = \frac{1}{\Gamma\left(\frac{1}{1+\alpha}\right)^{\frac{1-\alpha}{\alpha}} \cdot \Gamma\left(\frac{2}{1+\alpha}\right)}$$

for $\alpha = \frac{1}{7}$ we get $c = 0.654$ (3.22)

Trajectory Equation - From equations (3.16) and (3.19) the trajectory equation can be written as

$$\frac{d\bar{z}}{d\bar{x}} = \kappa^2 \left[\ell n \frac{k u_* t}{z_o e^{\gamma+1}}\right]^{-1}$$

or

$$\bar{x} = \frac{\bar{z}}{\kappa^2} \left[\ell n \frac{\bar{z}}{z_o e^{\gamma+1}}\right] \quad \text{for } \bar{z} > z_o e^{\gamma+1}$$

$$\frac{\kappa^2 \bar{x}}{z_o} = \frac{\bar{z}}{z_o} \left[\ell n \frac{\bar{z}}{z_o} - \gamma - 1\right] \tag{3.23}$$

3.5. The First Few Statistical Properties of the Cloud

The procedure adopted by Chatwin [1968], namely, "Aris moment transformation" is followed for determining the statistical properties of a cloud of material released instantaneously in a turbulent shear layer. Lagrangian similarity hypothesis is utilized in solving the equation (3.18) for the concentration field in space and time.

Equations (3.13) and (3.16) show

$$\chi_*(z,t) = \frac{1}{\kappa u_* t} \exp\left(-\frac{z}{\kappa u_* t}\right)$$

and $\qquad \bar{z} = \kappa u_* t$.

Vertical variance of the cloud can be obtained as

$$\sigma_z^2(t) = \int_0^\infty (z-\bar{z})^2 \chi_*(z,t)\, dz = (\kappa u_* t)^2 \quad . \tag{3.24}$$

In the constant stress layer where the turbulent intensities are of the same order as reported by Panofsky [1970], and Klebanoff [1955], the following assumption can be made.

$$\sigma_x^2 \propto \sigma_z^2 \propto (u_* t)^2 \quad .$$

The above results and the following Lagrangian hypothesis aid in tracking the solution for the equation (3.13). On dimensional grounds Batchelor [1964] has shown the solution of this equation as

$$\chi(x,z,t) = \frac{1}{a\kappa (u_* t)^2} F\left(\frac{x-\bar{x}}{a u_* t}, \frac{z}{\kappa u_* t}\right) \quad . \tag{3.25}$$

Now defining the similarity variables as

$$\beta = \frac{x-\bar{x}}{a u_* t} \quad \text{and} \quad \eta = \frac{z}{\kappa u_* t} \quad . \tag{3.26}$$

equation (3.18) is transformed to (see Appendix pages 53,54)

$$\eta \frac{\partial^2 F}{\partial \eta^2} + (\eta+1) \frac{\partial F}{\partial \eta} + \left(\beta - \frac{1}{a\kappa} \ln \eta e^{\gamma}\right) \frac{\partial F}{\partial \beta} + 2F = 0 \; . \tag{3.27}$$

This equation is in a convenient form to determine the statistical properties of the density function F. Moments of 'F' about $\bar{x}$ are defined as

$$\theta_n(\eta) = \int_{-\infty}^{\infty} \beta^n \, F \, d\beta \qquad \text{for} \quad n = 0,1,2,\ldots n. \tag{3.28}$$

$\theta_n(\eta)$ is the nth moment about the center of mass of the cloud. Boundary conditions to be satisfied by 'F' and $\theta_n(\eta)$ are:

$$F \to 0 \quad \text{as} \quad \beta \to \pm\infty$$

$$\text{and} \quad \eta \to \infty$$

$$\theta_n(\eta) \to 0 \text{ as } \eta \to \infty \quad n = 0,1,2\ldots$$

$$\eta \frac{d\theta_n}{d\eta} \to 0 \text{ as } \eta \to 0 \tag{3.29}$$

Multiplying the equation (3.27) by 1, β, β^2, $\beta^3,\ldots,\beta^n$ respectively and then integrating, using the boundary conditions (3.29), the following differential equations are obtained for the moments.

$$\eta \frac{d^2\theta_o}{d\eta^2} + (\eta+1) \frac{d\theta_o}{d\eta} + \theta_o = 0 \tag{3.30a}$$

$$\eta \frac{d^2\theta_1}{d\eta^2} + (\eta+1) \frac{d\theta_1}{d\eta} = - \frac{\theta_o}{a\kappa} \ell n \; \eta \; e^{\gamma} \tag{3.30b}$$

$$\eta \frac{d^2\theta_2}{d\eta^2} + (\eta+1) \frac{d\theta_2}{d\eta} - \theta_2 = - \frac{2\theta_1}{a\kappa} \ell n \; \eta \; e^{\gamma} \tag{3.30c}$$

$$\eta \frac{d^2\theta_3}{d\eta^2} + (\eta+1) \frac{d\theta_3}{d\eta} - 2\theta_3 = - \frac{3\theta_2}{a\kappa} \ell n \; \eta \; e^{\gamma} \tag{3.30d}$$

$$\vdots$$

$$\eta \frac{d^2\theta_n}{d\eta^2} + (\eta+1) \frac{d\theta_n}{d\eta} - (\eta-1)\theta_n = - \frac{n\theta_{n-1}}{a\kappa} \ell n \; \eta \; e^{\gamma} \tag{3.30e}$$

Solutions for $\theta_o(\eta)$ and $\theta_1(\eta)$ are obtained by P. C. Chatwin [1968] as

$$\theta_o(\eta) = e^{-\eta} \tag{3.31}$$

and $$\theta_1(\eta) = \frac{e^{-\eta}}{a\kappa}\,[\ell n\ \eta + \gamma - 1] + \frac{E_1(\eta)}{a\kappa} \tag{3.32}$$

where $E_1(\eta)$ is exponential integral given by

$$E_1(\eta) = \int_{\eta}^{\infty} \frac{e^{-\eta}}{\eta}\, d\eta$$

3.6. Dispersion Integral Equation

The author's major contributions are made in this section. The dispersion integral equation has been derived from the Eulerian equation of dispersion. This equation is solved to determine the second moment and its variation with height above the ground. Variance of the longitudinal density function is obtained for each horizontal layer of the cloud, from the distribution of second and first moments. This is an important statistical property of a dispersing cloud, which is directly related to the width of the cloud. The mean and the variance of a density function in each horizontal layer of the cloud are necessary to make quantitative estimates about concentration levels in a dispersing cloud. Such statistical properties are derived in this section for an instaneous line source in the surface shear layer. These estimates are not available in previous published works.

Substituting the expressions for $\theta_1(\eta)$ from (3.32) into equation (3.30c) we obtain the dispersion integral equation:

$$\eta\,\frac{d^2\theta_2}{d\eta^2} + (\eta+1)\,\frac{d\theta_2}{d\eta} - \theta_2 = \frac{-2}{a^2\kappa^2}\ \ell n\ \eta e^{\gamma}\ [e^{-\eta}(\ell n\ \eta+\gamma-1) + E_1(\eta)] \tag{3.33a}$$

Multiplying (3.33) by $(\eta+1)\,e^{\eta}$ and integrating we obtain

$$(\eta+1)\,\frac{d\theta_2}{d\eta} - \theta_2 = -\frac{2}{a^2\kappa^2}\,\Big[\frac{E_1(\eta)+\ell e^{-\eta}}{\eta}\,(\eta\ell-1) + \eta e^{-\eta}\frac{(\ell-1)^2}{2} - 2e^{-\eta}(\ell-1)\Big] \tag{3.33b}$$

where $\ell = \ell n(\eta e^{\gamma})$ (see Appendix pages 54-56).

Now it can be shown that (see Appendix pages 56-57).

$$\theta_2(\eta) = \frac{2(\eta+1)}{a^2\kappa^2} \int_{\eta}^{\infty} \left[\frac{E_1(\eta)+\ell e^{-\eta})(\eta\ell-1)}{\eta(\eta+1)^2} + \frac{\eta e^{-\eta}(\ell-1)^2}{2(\eta+1)^2} - \frac{2e^{-\eta}(\ell-1)}{(\eta+1)^2}\right] d\eta \tag{3.33c}$$

This integration has been performed, term by term using the boundary conditions (3.29). It is shown that (see Appendix pages 57-59),

$$\theta_2(\eta) = \frac{1}{a^2\kappa^2} [2E_1(\eta)\ell + \ell^2 e^{-\eta}(\eta+2)-2\eta E_1(\eta) + 3e^{-\eta}-(\eta+1)(\Gamma''(1,\eta) + 2\gamma\Gamma'(1,\eta) + \gamma^2 e^{-\eta})] \tag{3.34}$$

where $$\Gamma''(1,\eta) = \int_{\eta}^{\infty} e^{-t} (\ell n\ t)^2\, dt ,$$

$$\Gamma'(1,\eta) = \int_{\eta}^{\infty} e^{-t}\ \ell n\ t\, dt , \text{ and}$$

$$\Gamma^n(a,\eta) = \frac{\partial^n \Gamma(a,\eta)}{\partial a^n} = \int_{\eta}^{\infty} (\ell n\ t)^n e^{-t}\, t^{a-1}\, dt$$

are the derivatives of incomplete gamma functions w.r.t. the parameter 'a'. These derivatives were obtained by the author for all 'n' (see Appendix pages 70-72).

$$\Gamma''(1,\eta) = \int_{\eta}^{\infty} e^{-\eta} (\ell n\ \eta)^2\, d\eta$$ is not tabulated elsewhere

to the author's knowledge and is difficult to evaluate as such. This integral was transformed as shown in Appendix, page 71 to evaluate it,

$$\int_{\eta}^{\infty} e^{-\eta} (\ell n\ \eta)^2\, d\eta = \Gamma''(2,\eta) - \eta e^{-\eta}(\ell n\ \eta)^2 - 2\Gamma'(1,\eta)$$

where

$$\Gamma''(2,\eta) = \int_{\eta}^{\infty} \eta e^{-t} (\ell n\ \eta)^2\, d\eta = \int_{0}^{\infty} e^{-\eta}(\ell n\ \eta)^2\, d\eta - \int_{0}^{\eta} \eta e^{-\eta}(\ell n\ \eta)^2\, d\eta$$

$$= \frac{\pi^2}{6} + \gamma^2 - 2\gamma - \int_{0}^{\eta} \eta\ e^{-\eta} (\ell n\ \eta)^2\, d\eta \quad .$$

The second integral was performed numerically by utilizing Romburg's iteration technique, correcting the end points to the eighth decimal place. They were tabulated by the author for the value of 'η' equal to 10.0 with an interval of 0.001.

$\theta_2(\eta)$ has the following properties

at $\eta = 0$ $\quad \theta_2(\eta) = \dfrac{1}{a^2\kappa^2}\left[3 - \dfrac{\pi^2}{6}\right]$ (see Appendix page 60)

as $\eta \to \infty$ $\quad \theta_2(\eta) \to 0$ (Appendix Page 60)

and $\displaystyle\int_{0}^{\infty} \theta_2(\eta)\, d\eta = \frac{1}{a^2\kappa^2}\left[\frac{\pi^2}{6} - 1\right]$ (see Appendix page 61) (3.35)

In obtaining the above integrals we utilize the following property:

$$[E_1(\eta) + e^{-\eta}\ \ell] \to 0 \quad \text{as} \quad \eta \to 0$$

Reference can be made to the tables referred to in the bibliography.

Numerical values of $\theta_2(\eta)$ were obtained utilizing the above results. The nature of $\theta_2(\eta)$ with increasing height was shown in Fig. 2. The mean and variance of the density function for the direction of mean flow can now be derived as follows.

$$x_m = \mu(\eta) = \frac{\int_{-\infty}^{\infty} x\ \chi\ dx}{\int_{-\infty}^{\infty} \chi\ dx}$$

Transforming the variables as shown

$$x = au_*t\ \beta + \overline{x}\ , \qquad \chi = \frac{1}{a\kappa(u_*t)^2}\ F(\beta,\eta)$$

it can be shown that

$$\int_{-\infty}^{\infty} \chi\ dx = \int_{-\infty}^{\infty} \frac{1}{\kappa u_*t}\ F d\beta = \frac{\theta_o(\eta)}{\kappa u_*t}\ ,$$

$$\int_{-\infty}^{\infty} x\ \chi\ dx = \frac{a}{\kappa}\ \theta_1(\eta) + \frac{\overline{x}\theta_o(\eta)}{\kappa u_*t}\ ,$$

and

$$\mu(\eta) = (au_*t)\ \frac{\theta_1(\eta)}{\theta_o(\eta)} + \overline{x}\ . \tag{3.36}$$

Similarly,

$$\sigma_x^2(\eta) = \frac{\int_{-\infty}^{\infty} (x-\mu)^2\ \chi dx}{\int_{\infty}^{\infty} \chi\ dx} = (au_*t)^2 \left[\frac{\theta_2(\eta)}{\theta_o(\eta)} - \left(\frac{\theta_1(\eta)}{\theta_o(\eta)}\right)^2\right] \tag{3.37}$$

Figures (3) and (4) show the results, μ and σ_x^2 as a function of η. They show that the variance of the cloud remains approximately as constant with height in the region of the boundary layer under consideration. This result follows the constancy of the shear stress in the surface layer.

3.7. Skewness Properties of the Cloud

Solution of the equation (3.30) for the third central moment will reveal the skewness properties of the density function for the direction of mean flow at all planes above the boundary.. Multiplying the equation (3.30d) by $e^{\eta}(\eta^2+4\eta+2)$ for convenience and integrating it can be shown (see Appendix pages 62-63).

$$(\eta^2+4\eta+2)\frac{d\theta_3}{d\eta} - 2(\eta+2)\theta_3 = -\frac{3}{a\kappa}\frac{e^{-\eta}}{\eta}\int_0^{\eta}\theta_2 e^{\eta}\,\ell\,(\eta^2+4\eta+2)d\eta \quad . \tag{3.38}$$

Integration of this equation (3.38) between the limits of zero and infinity using the boundary conditions (3.29) leads to

$$2\theta_3(0) + 4\int_0^{\infty}\eta\theta_3 d\eta + 8\int_0^{\infty}\theta_3 d\eta = \frac{3}{a\kappa}\int_0^{\infty}\frac{e^{-\eta}}{\eta}\left[\int_0^{\eta}\theta_2 e^{\eta}\,\ell(\eta^2+4\eta+2)d\eta\right]d\eta \quad . \tag{3.39}$$

The integral on the right hand side of the equation (3.39) is complicated for analytical work. It has been solved by numerical methods to obtain the following value (This result is shown in Fig. 7). Now it can be shown that

$$\theta_3(0) = \frac{1}{2a^3\kappa^3}\left[5.715 - 4\int_0^{\infty}\eta\,\theta_3(\eta)d\eta - 8\int_0^{\infty}\theta_3(\eta)d\eta\right] \quad . \tag{3.40}$$

To obtain the values of the second and third integrals on the right hand side of the equation (3.40), multiply the equation (3.30d) by unity and 'η' respectively and integrate them between the limits of zero and infinity. Using the boundary conditions (3.29), it can be shown that (see Appendix pages 64-70).

$$\int_0^{\infty}\theta_3 d\eta = \frac{1}{a\kappa}\int_0^{\infty}\ell\,\theta_2\,d\eta = \frac{1}{a^3\kappa^3}\left[4 - \frac{\pi^2}{6} + \psi''(1)\right]$$

and
$$\int_0^{\infty}\eta\theta_3 d\eta = \frac{1}{4}\left[\int_0^{\infty}\theta_3 d\eta + \frac{3}{a\kappa}\int_0^{\infty}\eta\,\ell\,\theta_2 d\eta\right]$$

$$= \frac{1}{4a^3\kappa^3}\left[\left(4 - \frac{\pi^2}{6} + \psi''(1)\right) + 3\left(2\frac{\pi^2}{6} - \frac{5}{9} + \frac{11}{9}\psi''(1)\right)\right]$$

$$\simeq -0.15979/a^3\kappa^3 \tag{3.41}$$

Substituting these values in equation (3.40), it can be shown that

$$\theta_3(0) \approx - \frac{2.267}{a^3\kappa^3} \quad . \tag{3.42}$$

The skewness coefficient of the density function is given by

$$\lambda_3(\eta) = \frac{E[(x-x_m)^3]}{[E(x-x_m)^2]^{3/2}} = \frac{1}{\sigma^3(z,t)} \frac{\int_{-\infty}^{\infty} (x-x_m)^3 \chi \, dx}{\int_{\infty}^{\infty} \chi \, dx}$$

$$= \left[\frac{\theta_3(\eta)}{\theta_o(\eta)} + 2\left(\frac{\theta_1(\eta)}{\theta_o(\eta)}\right)^3 - 3\frac{\theta_1(\eta)\theta_2(\eta)}{\theta_o^2(\eta)} \right] \Bigg/ \left[\frac{\theta_2(\eta)}{\theta_o(\eta)} - \left(\frac{\theta_1(\eta)}{\theta_o(\eta)}\right)^2 \right]^{3/2} \tag{3.42}$$

At ground level the value of $\eta = 0$. Substituting the values for $\theta_3(0)$, $\theta_2(0)$, $\theta_1(0)$, $\theta_o(0)$ in the equation (3.42), the skewness coefficient at the ground level can be obtained as

$$\lambda_3(0) = - \frac{0.215}{(0.355)^{3/2}} = - 1.02 \quad . \tag{3.43}$$

Further integration of the equation (3.38) to obtain the skewness coefficient as a function of height has been found to be unnecessary. This effect is discussed in Section 4.1.3.

CHAPTER IV

RESULTS AND DISCUSSIONS

In this chapter, the statistical properties of dispersion of materials released from an instantaneous line source are discussed. Based on these properties, namely the mean, variance and skewness coefficient, a descriptive field of concentrations and a probable shape of the cloud are presented. Spatial distribution of material due to a quasi-continuous source, and ground level concentrations downwind of a continuous line source are also presented. The results for a continuous line source are compared with the available data.

4.1. Discussion of the Statistical Properties of the Cloud

In this section, the mean, variance and the skewness properties of the cloud are presented. Mean and variance of the longitudinal distribution of the material within the cloud are found to vary with height above the boundary. They also vary with time of flight of the cloud. An expression derived for the variance shows qualitative agreement with the existing experimental results.

4.1.1. Mean of the concentration distribution - Mean of the concentration distribution is defined in the context of the present work as, the mean of longitudinal distribution of the material in a horizontal layer of the cloud parallel to the surface. This mean is a function of height above the surface and increased with height. Variation of the mean with height is discussed in this section.

Mean of the concentration distribution is given in equation (3.36) as

$$x_m = \frac{\int_{-\infty}^{\infty} x\chi dx}{\int_{-\infty}^{\infty} \chi dx} = au_* t \frac{\theta_1(\eta)}{\theta_o(\eta)} + \bar{x} \tag{4.1}$$

Variation of the mean with height is shown in Fig. 3, with the following nondimensional coordinates.

$$\psi = \frac{x_m - \bar{x}}{u_* t/\kappa} \quad \text{and} \quad \eta = \frac{z}{\kappa u_* t} \tag{4.2}$$

Mean coincides with the center of mass at a height where $\eta = 0.7362$. Above this characteristic height, the could leads its center of mass, and below this height it lags behind the center of mass. This variation of mean with height introduces profound skewness in the shape of the cloud, which will be discussed in Section (4.3). Velocity gradient present in the surface layer is primarily responsible for this nonsymmetry in the shape of the cloud.

4.1.2. <u>Variance of the cloud</u> - For any passive matter released in a two dimensional turbulent shear flow, the center of mass of the cloud of material disperses in two directions. The cloud disperses and diffuses around the center of mass due to shear, turbulent and molecular diffusion properties of the characteristic flow field. Variance of a diffusing cloud of contaminant in a turbulent shear flow characterizes these properties. G.I. Taylor [1921] demonstrated that the variances are related to the Lagrangian correlation function of turbulent motion. These functions are not established due to inherent difficulties involved in obtaining them. However, variances are obtained in this present work (Section 3.6) by assuming Lagrangian similarity for the solutions of Eulerian equations of turbulent dispersion.

Variance of the cloud for the vertical direction was given in equation (3.24) as

$$\sigma_z^2 = E[z-\bar{z}]^2 = (\kappa u_* t)^2 \tag{4.3}$$

Variance for the longitudinal direction of the cloud was obtained in equation (3.37) as a function of height. Variation of this variance with height is presented in Fig. 4, on a nondimensional coordinate plane. In a horizontal plane, variance increased proportionally to the square of time. At any given time variance increased slowly with height up to $\eta = 2.75$ and then decreased monotonically. These properties are similar to those of longitudinal oscillations $\overline{u'^2}$ or turbulent shearing stress in a two dimensional turbulent shear flow [Klebanoff, P.S., 1955].

Rate of variation with height of the longitudinal variance was very small within the height of the surface layer of the atmosphere. Hence it was assumed to be a constant for the computation of the concentration field.

4.1.3. Skewness property of longitudinal density function - Skewness properties of a diffusing cloud were treated analytically in Section 3.7. Skewness coefficient for the longitudinal density function was expressed by the equation (3.42). This coefficient was obtained for ground level distribution. It was assumed to remain constant within the height of the surface layer of atmosphere for the following reasons: Lagrangian similarity is assumed for the solution of a two-dimensional dispersion equation in the present analysis. This similarity hypothesis results in providing a density function for the concentration, which remains similar for all points in space. Skewness coefficient is a nondimensional parameter which should remain constant, since the density function should remain similar for all space-time configurations.

Shape of an instantaneous line source, a descriptive field of concentrations for a quasi continuous source and ground level concentrations for a continuous line source are presented in the following sections, treating the skewness coefficient as a constant.

4.2. Density Function for Concentration

Exact solutions obtained in Chapter III for the statistical properties of the cloud allowed us to specify the density function. This is obtained by truncating the derived density function (3.13) to the third Hermite polynomial and substituting the statistical parameters as shown.

$$\chi(x,z,t) = \frac{A}{\sqrt{2\pi}\,\sigma_x \sigma_z} \left[1 - \frac{1}{6}(\xi^3 - 3\xi)\right] \mathrm{Exp}\left(-\frac{\xi^2}{2} - \frac{z}{\kappa u_* t}\right)$$

σ_x^2 = Variance of longitudinal density function, given by Eq. (3.37)

σ_z^2 = Variance of marginal density function, given in Eq. (3.24)

$\xi = (x - x_m)/\sigma_x$

A = 1.01 is a constant, makes the density integrate to unity.

A typical density curve for the concentration at ground level is presented in Fig. 6 . However, the concentrations at other levels above the ground can be obtained from the same figure. The density curve may be slid along the mean curve to a required height, 'η' , and multiplied by the marginal density function, '$e^{-\eta}$' . Concentration versus time curves can also be obtained from the above density function.

4.3. Shape of the Instantaneous Line Source Cloud

The shape of line source cloud was obtained from the descriptive field of concentrations. A typical shape of the diffusing cloud is given in Fig. 7, employing similarity coordinates. The shape is given by isocontour lines; these contour lines beyond the 10 percent line exhibit a hump at the back of the cloud. The reason for such a behavior is explained as the effect of truncation of the density function. Apparantly the truncation does not give a good approximation at the tail of the longitudinal density function.

A cross-section of the cloud is found to be asymmetric about its mean. This effect is due to the presence of profound shear in the surface layer of the atmosphere. The top of the cloud is stretched forward with a greater speed while it is simultaneously diffusing in the vertical and longitudinal directions. Experimental verification of these properties is possible by using photographic techniques. However, it is extremely difficult to design instrumentation which can collect and measure the instantaneous concentrations. Samples of measurable concentration are difficult to obtain while the cloud is diffusing and simultaneously convecting rapidly in a turbulent atmosphere. Chandra [1968] measured the instantaneous concentrations and obtained the cross-section of a point source cloud. In his experiments the uncertainty in the measurements was explained by the distortion and compression effects of the diffusing cloud in the sampling tubes. There is no report available on the longitudinal distribution of the material.

The variances obtained in equation (3.24) and (3.37) reflect the gross characteristics of the diffusing cloud. Experimental results on variance of instantaneous sources have been reported by Frenkiel and Katz [1956]. They concluded from their field data that particle variances for instantaneous sources are proportional to the square of the time of their travel. Sources were released at various heights within the first one hundred meters of the planetary boundary layer. Gifford's analysis [1957] based on Kellogg's [1956] data also supports the above conclusions, i.e., the variances of the dispersing puffs are proportional to the square of the dispersion time.

4.4 Quasi-Continuous Source

Instantaneous source is a fictitious one, in which the contaminants have to be released within a zero interval of time. Such a source does not exist in practice. Most of the sources in practice are quasi-continuous. Dispersion of matters due to such sources cannot be easily treated analytically. However, semianalytical predictions can be made for these sources, by integration of the distribution function of an instantaneous source, for their total life time.

Equation (3.33) is integrated numerically for a specified time of release and the results obtained are presented in Figs. 8, 9 and 10. In these figures spatial distribution of the material is shown in real coordinates. The concentration curves are extremely nonsymmetrical due to shear effects in the surface layer. These figures indicate that there is a horizontal layer in which the concentration remains constant with distance downstream. On the other hand, in the layers below this, the concentration decreases with increasing distance. In the layers above this, the concentration increases with downwind distance. These results can be visualized better when the lifetime of the source is increased. Computer programs, to obtain these spatial distribution curves, are given in Appendix II.

Plume height can be predicted from the isoconcentration lines of a prolonged quasi-continuous source. However, an optical threshhold on the density of the plume has to be defined in such cases.

Experimental verification of predictions made about quasi-continuous source is possible under careful instrumentation techniques. In some experiments dosages were measured for elevated instantaneous line sources. MacCready, Smith and Wolf [1961] reported the results for sources released from a low flying aircraft. Similar experimental results were reported by Smith and Wolf [1963]. In all these cases, sources were located at heights beyond the surface layer and dosages at ground level were measured. No data was reported of the instantaneous distribution of the material. The marked effect of irregular terrain on diffusion patterns is also reflected in these experiments. The data shows a large scatter and offers little help in establishing any theoretical development. Experiments under controlled conditions are not available. Such experimental results can be obtained only in wind tunnel studies. Sophisticated instrumentation capable of measuring instantaneous concentrations are still in a development stage. Progress on instrumental techniques to measure the concentrations of a diffusing cloud are reported by Lumley [1970].

4.5. Monin-Pasquill's Constant b'

Monin [1959] proposed a similarity relation for dispersion in neutral flows, to determine the extent of vertical spread of smoke within the surface layer. He defined

$$\omega^* = \frac{dz_{max}}{dt} = b' u_* \tag{4.5}$$

He reported a value for $b' = 0.75$ by analyzing his experiments on smoke puffs. The R.M.S. value of vertical components of wind velocity was shown to be

$$\sqrt{\overline{w'^2}} = 0.86\ u_* \tag{4.6}$$

Pasquill [1966] obtained a value of $b' = 1.2$ on the analysis of experimental data at Porton. However, in his analysis he defined z_{max} as the height at which the concentration level $\chi = 0.1\ \chi_{max}$. Such an assumption for z_{max} is essential to avoid any specification of optical threshold and visibility conditions in the field.

In the present theoretical analysis, the value of b' is estimated. Utilizing the results in Fig. 7, and defining z_{max}, the same way as Pasquill did, i.e., the value of b' is estimated as follows:

$$\frac{z_{max}}{\kappa u_* t} = 2.3 \quad \text{at} \quad \chi = 0.1\ \chi_{max} \tag{4.7}$$

$$z_{max} = 2.3\ \kappa u_* t \tag{4.8}$$

$$\frac{\partial z_{max}}{\partial t} = 2.3\ \kappa u_* = 0.92\ u_* = b' u_* \tag{4.9}$$

Hence $\qquad b' = \underline{0.92}$.

This value of b' lies in between the experimental estimates of Monin and Pasquill.

4.6. Cloud-Length at the Ground Level

The length of a diffusing cloud of an instantaneously released mass at ground level is defined as follows: It is the range of distance at the ground level which is exposed to the contaminant by at least 10 percent of the maximum concentration level present in the cloud at any given time after release. Length increases with time or distance of travel of the cloud. This length is obtained from Fig. 7 by the 10 percent isoconcentration line as

$$W = \frac{x_1 - x_m}{a u_* t} - \frac{x_2 - x_m}{a u_* t} = \frac{x_1 - x_2}{a u_* t} = \frac{4.35}{a u_* t} \tag{4.10}$$

where $\frac{x_1 - x_m}{a u_* t}$ and $\frac{x_2 - x_m}{a u_* t}$ are the points of intersection of the 10 percent concentration line at the ground level.

This distance can be related to the mean distance traveled by the cloud at the ground level as follows: From (3.36) it can be shown that,

$$x_m \Big|_{z=0} = \frac{u_* t}{\kappa} + \bar{x} \tag{4.11}$$

Using the expression for $\bar{x}$ from equation (3.20) it can be written that

$$\begin{aligned} x_m \Big|_{z=0} &= \frac{u_* t}{\kappa} \left[\ell n \frac{\kappa u_* t}{z_o} - \gamma - 2\right] \\ &= \frac{u_* t}{\kappa} \ell n \frac{\kappa u_* t}{z_o e^{\gamma+2}} \end{aligned} \tag{4.12}$$

and

$$\frac{x_m}{W} = \frac{1}{4.35\ a\kappa} \ \ell n \left(\frac{\kappa u_* t}{z_o e^{\gamma+2}}\right) \tag{4.13}$$

where $a \approx 1.5$

$\kappa = 0.4$

4.7. Ground Level Concentrations Due to a Continuous Line Source

In order to obtain the ground level concentrations for a continuous line source, numerical integration of density function with respect to time was performed in the computer CDC 6400 at Colorado State University. Here stationary conditions were assumed for the turbulent flow field.

Writing the ground level concentration for continuous line source as:

$$\chi_{c\ell}(x,z)\Big|_{z=0} = \int_{o}^{t_1} \chi(x,z,t)dt + \int_{t_1}^{t_2} \chi(x,z,t)dt + \int_{t_2}^{\infty} \chi(x,z,t)dt \qquad (4.14)$$

the numbers 't_1' and 't_2' were found such that the contribution from the integrals one and three on the right hand side of the above equation were negligible. Hence, the integration was performed for the interval of time between t_1 and t_2 only. This truncation reduced the computing time considerably. Integration performed for any further length of time contributed no significant increase of accuracy. The time interval chosen for the integration was an optimum one, so that steady state answers were obtained. A smaller interval did not produce any significant deviation.

Ground level concentrations were obtained for different topographical conditions by varying the roughness coefficient 'z_o'. Concentrations were also computed for different values of mean velocity. This was done by varying the values of shear velocity. These results are shown in Fig. 12. Concentrations at different sites downstream of a continuous line source gave a definite relationship between the shear velocity, roughness coefficient and downwind distance as

$$\chi_{c\ell}(x,z)\Big|_{z=0} \propto \frac{1}{u_* z_o^m x^p} \qquad (4.15)$$

It was found that exponent $m \approx 0.1$. The exponent 'p' varied with location. For value of 'x' of the order 10^n feet, 'p' increased as 'n' increased and reached an asymptotic value of one for large 'n' of the order of four. This asymptotic value for 'p' was predicted by Batchelor [1964].

Continuous line source experiments in the wind tunnel by Poreh [1963] and Quarashi [1963] compare well with the present results of the exponent 'p'. Field experiments at Porton, reported by Pasquill [1962] gave values for the exponent 'p' in the range of 0.9 - 1.0 .

4.8. Qualitative Comparison Between the Observations in the Atmosphere and the Results Obtained by the Similarity Theory

Observations made in the atmosphere on the dispersion of radioactive materials released from instantaneous and quasi-continuous point sources are available from the atomic energy publication by P.W. Nickola *et al.*, [1970]. Instantaneous sources were simulated by crushing glass ampules filled with Kriplon-85 gas, by rifle shots. Experiments were conducted on a flat terrain under various stability conditions in the atmosphere. Data were collected for mean velocity, temperature distribution, standard deviation of wind speed and direction. Ground level concentrations were obtained at 200 m. and 800 m. from the source by radioactive detectors. Data stored and printed by computer are available. Basically speaking, this data cannot be used as such for comparison, because observations are made for instantaneous point source and the theoretical development in this study is for an instantaneous line source. However, if the assumption is made that the flow is laterally homogeneous, it is possible to integrate the data for lateral direction to represent line source data.

Test number P5 has been selected from the eight tests conducted for instantaneous sources, because the velocity distribution of wind was very nearly logatithmic during this test in the field. Velocity distribution plotted on a semi-logarithmic paper provided a best fit, giving the values of shear velocity $u_* = 0.836$ m/sec and roughness coefficient $z_o = 0.0536$ m. Substituting these values into (3.13), (3.16) and (3.20), the marginal density and center of mass of the cloud were obtained for the dispersing material for any given time after release. These results are shown in Fig. 13. Observations on the ground level exposers of material are also shown in this figure. It can be seen from this figure that there is not promising agreement between the predictions and observations. Reasons for this disagreement were, however, investigated. End window type detectors were used as sensors to measure the instantaneous concentrations in a dispersing cloud of radioactive gas. These detectors were calibrated in the gas enclosed in a balloon. Calibration provides a relation between the concentration and the number of counts per second. However, when these detectors are placed in a dispersing cloud, they may count less than they could have counted in a stationary cloud of the same concentration. Secondly, the observations reported are not for instantaneous concentrations. They are for an average over 2.4 seconds. When the cloud is convecting and diffusing, the measured average will be less than the instantaneous concentration present at any spatial point. Also, stability of the atmosphere was slightly unstable during this test. Such a stability condition enhances the vertical transfer and reduces the ground level exposures when compared to the adiabatic atmosphere. The above reasoning indicates that the theoretical estimates would be expected to be higher compared to the experiments. Estimation of errors due to calibration defects and unstableness of the flow are possible when details about the flow and complete description of the concentration field are known. Such details are not available. However, it can be seen that the time of peak ground level exposure has been well predicted. Given a distance, 'x' , from the source, exposure time of the contamination at ground level can also be well predicted when the distribution of wind is known.

Observations about the dispersion of instantaneous point sources within the first one hundred meters of the atmosphere were also reported by Frenkiel and Katz [1953]. By analyzing the visual diameters of dispersing smoke puffs, they concluded that the particle variances were proportional to the square of time of their travel. Gifford's [1957] analysis, based on Kellogg's [1956] data, also concludes that the variances of concentration within the dispersing puffs are proportional to the square of time of dispersion. In the present work, variance characteristics of the instantaneous line source were derived from the semi-empirical equation of dispersion by utilizing the Lagrangian similarity hypothesis. Results shown in equation (3.24) and (3.37) are in agreement with the above conclusion drawn from field observations.

4.9. Practical Applications of the Investigation

The investigation reported in the present study is mainly oriented towards understanding the effect of the dispersion of pesticides and insecticides, released by aircrafts, on vegetation in farm lands and forest areas. It is very important to estimate the ground level exposures due to the spread of these materials. Excessive exposures are very dangerous. Recent studies on food quality indicate that an excess use of pesticides and insecticides are responsible for food poisoning. If they are present in excess they may be absorbed by plants during osmotic processes and inspiration. They may also enter food products by direct contact. So it is very important to understand the mechanism of spread of these materials in order to provide reliable estimates of ground level exposures. These materials are always released across the direction of the wind to ensure even spread and maximum coverage of land. Such a source can be well represented by an instantaneous line source. The present study has accomplished in providing a primary solution for the spread of materials released from such a source when the density of the material is not very much different than the density of air. Ground level exposures can be easily estimated when the distribution of wind velocity is known. Such estimates can be used to set standards on the strength of the releases to ensure not exceeding allowable exposure levels on the vegetation.

This study can also be used to estimate ambient air pollution levels from automobile exhausts, when the wind direction is across the highway system. Automobiles release exhaust gases at ground level. When the wind blows across the highway, these releases from each automobile can be treated as a separate instantaneous line source. Distribution of the material released from each source can be obtained using the proposed density function in the present study. However, when the frequency of the automobiles and their corresponding strength of releases is known, pollution level downwind of the highway due to the automobiles can be estimated by summation of the contribution from each automobile at any given location. Such estimates can be easily obtained using the present high speed computers.

CHAPTER V

CONCLUSIONS

1. Dispersion of mass from an instantaneous line source, in the atmospheric surface layer is investigated. An exact solution for the marginal density function is obtained from the Eulerian equations of dispersion. This function gives the exact amount of material present in each horizontal layer of the dispersing cloud, at any time after release.

2. Moment equations are derived from the Eulerian equations by assuming Lagrangian similarity density function for concentration field. These equations are solved to obtain the statistical properties, namely the mean, the varinace and the skewness coefficient of the longitudinal density function. The vertical distribution of the variance property of the cloud indicates a striking similarity with the distribution of shear stress in the surface layer of the atmosphere.

3. The Gram-Charlier density is shown to be suitable for the longitudinal distribution of the material. Substituting the statistical properties into this function a longitudinal density function is developed.

4. Utilizing these density functions, spacial distribution of concentration is obtained. The shape of the cloud is obtained by drawing the isoconcentration lines. The cloud is found to be asymmetrical with the upper layers of the cloud pulled more in the direction of wind than the lower layers.

5. The maximum height of the cloud is found to be increasing linearly with time. The proportionality constant b' in the relation $Z_{max} = b'u_* t$, has been found to be equal to 0.92. This value lies in between the experimental observations of Monin [1959] and Pasquill [1966].

6. The length of the cloud is found to be always greater than the height. The length to height ratio, which can be obtained as the ratio of the two standard deviations σ_x/σ_z is shown to be equal to 3.75. This result is in good agreement with the experimental estimation of 4.0, obtained by Kazanski and Monin (Monin 1959).

7. It is demonstrated that the concentration field due to finite length releases can be obtained by the numerical integration of the density function for the total time of release. However, in such cases, stationary conditions are assumed for the flow.

8. The density function is integrated with respect to time to obtain ground level concentrations due to a continuous line source. These integrations are performed numerically for various downwind distances with different values for shear velocity u_* and roughness coefficient z_o. The results showed a systematic variation with u_* and z_o. A relation for the concentration decay rate is obtained as $\chi \propto \frac{1}{u_* z_o^m x^p}$. The value of 'm' is found to be 0.1 and the value of p is found to vary with the distance 'x'. For the values of 'x' of the order of 10^n feet, p increased as 'n' increased and reached an asymptotic value of 1.0 for 'n' or the order of four. This value is predicted by Batchelor [1964] by utilizing Lagrangian similarity principles. For values of 'n' in between 2 and 3 the value of p is found to be 0.92. This result

is in good agreement with the observations in wind tunnels and field experiments.

BIBLIOGRAPHY

BIBLIOGRAPHY

Batchelor, G. K., 1958. The theory of homogeneous turbulence: Cambridge University Press.

Batchelor, G. K., 1959. Note on the dispersion from sources in a turbulent boundary layer: (Unpublished).

Batchelor, G. K., 1964. Diffusion from sources in a turbulent boundary layer: Polaska Akadamia Nauk.

Cermak, J. E., 1963. Lagrangian similarity hypothesis applied to diffusion in turbulent shear flow: J. Fluid Mech., Vol. 15, Part 1, pp. 49-64.

Chandra, S., 1968. Dispersion of instantaneous point source: Dissertation at Colorado State University.

Chatwin, P. C., 1968. The dispersion of a puff of passive contaminant in a constant stress region: Quart. J. Roy Met. Soc., Vol. 94, No. 401, pp. 555-62.

Chaudhry, F., 1969. Turbulent diffusion in stably stratified flows: Dissertation at Colorado State University.

Ellison, T. H., 1959. Turbulent diffusion: Science Progress 47, pp. 495-506.

Frenkiel, F. N., 1959. A coment on Monin's paper: Advances in Geophysics, Vol. 5, p. 331.

Frenkiel, F. N., and Katz, I., 1956. Studies of small scale turbulent diffusion in the atmosphere: J. Met., Vol. 13, pp. 384-394.

Gifford, F. A., 1957. Relative atmospheric diffusion of smoke puffs: J. Met., Vol. 14, pp. 410-414.

Gifford, F. A., 1962. Diffusion in the diabatic surface layer: J. Geophysical Res., Vol. 67, No. 8, pp. 3207-3211.

Kellogg, W. W., 1956. Diffusion of smoke in the stratosphere: J. Met., Vol. 13, No. 3, pp. 241-250.

Klebanoff, P. S., 1955. Characteristics of turbulence in a boundary layer with zero pressure gradient: NACA Report 1247, Washington.

Klugg, W., 1968. Diffusion in the atmospheric surface layer. Comparison of similarity theory with observations: Quart. J. Roy. Met. Soc., Vol. 94, pp. 555-562.

BIBLIOGRAPHY - (Continued)

Longuet, Higgins M., 1963. The effect of non-linearations on statistical distribution in the theory of sea waves: J. Fluid Mech., Vol. 17.

Lumley, J. L., 1970. Prediction of the path of pollution particles: Mechanical Engineering (ASME), Vol. 92, No. 5.

MacCready, Smith and Wolf, 1961. Vertical diffusion from a low altitude line source: Met. Res. Inc., Vols. 1 and 2, Altadena, California.

Monin, A. S., 1959. Smoke propogation in the surface layer of atmosphere: Adv. in Geophysics, Vol. 6, p. 331.

Monin, A. S. and Yaglam, 1966. Statistical hydrodynamics: Clearing house publication No. JPRS: 37,763, TT: 66-34,191, Chapter V.9.4, p. 456.

Panofsky, H. A. and Prasad, B., 1965. Similarity theories and diffusion: Int. J. Air Wat. Pol., Vol. 9, pp. 419-430.

Pasquill, F., 1962. Atmospheric diffusion: D. Van Nostrand Co., London. Library of Congress catalog No. 61-13476.

Pasquill, F., 1966. Lagrangian similarity and vertical diffusion from a source at ground level: Quart. J. Roy. Met. Soc., Vol. 92, No. 392, pp. 185-195.

Poreh, M. and Cermak, J. E., 1963. Study of diffusion from a line source in a turbulent boundary layer: Int. J. Heat and Mass Transfer, Vol. 7, pp. 1083-1095.

Quarashi, A., 1963. Effects of flexible roughness elements on diffusion in a turbulent boundary layer: Ph.D. dissertation at Colorado State University.

Saffman, P. G., 1962. The effect of wind shear on horizontal spread from an instantaneous ground source: Quart. J. Roy. Met. Soc., Vol. 88, pp. 382-393.

Smith, T. B. and Wolf, M. A., 1963. Vertical diffusion from an elevated line source over a variety of terrains: Met. Res., Inc. Altadena, California.

Sutton, O. G., 1932. A theory of eddy diffusion in the atmosphere: Proc. Roy. Soc., London, A, 135, pp. 143-165.

Turner, Bruce D. Work book of atmospheric dispersion estimates: Public Health Service Publication No. 999-AP-26.

BIBLIOGRAPHY - (Continued)

Tables - Tables of Sine, Cosine and exponential Integrals, Vol. 1, Federal Works Agency. Works project administration for city of New York. 1940.

APPENDIX I

DERIVATION OF EQUATIONS APPEARED IN CHAPTER III

APPENDIX I

Derivation of Equation (3.27) in the Text

Consider the dispersion equation (3.18):

$$\frac{\partial \chi}{\partial t} + [\frac{u_*}{\kappa} \ell n \frac{z}{z_o}] \frac{\partial \chi}{\partial x} = \frac{\partial}{\partial z} (\kappa \; u_* \; z \frac{\partial \chi}{\partial z}) \qquad (3.18)$$

(1) (2) (3)

Equation (3.25) gives

$$\chi(x,z,t) = \frac{1}{a\kappa(u_* t)^2} \; F \; (\frac{x-\bar{x}}{au_* t} , \frac{z}{\kappa u_* t}) \qquad (3.25)$$

Substitutions from (3.26) and (3.20):

$$\beta = \frac{x - \bar{x}}{au_* t} \quad , \quad \eta = \frac{z}{\kappa u_* t} \quad , \quad \bar{x} = \frac{u_* t}{\kappa} [\ell n \frac{u_* t}{z_o e^{\gamma}} - 1]$$

From equation (3.25), the following relations are derived:

(1) $$\frac{\partial \chi}{\partial t} = \frac{1}{a\kappa u_*^2} (- \frac{2}{t^3}) F + \frac{1}{a\kappa(u_* t)^2} \frac{\partial F}{\partial \eta} (\frac{-z}{\kappa u_* t^2})$$

$$+ \frac{1}{a\kappa(u_* t)^2} \frac{\partial F}{\partial \beta} [- \frac{x}{au_* t^2} - \frac{1}{au_* t} \{\frac{u_*}{\kappa} [\ell n \frac{\kappa u_* t}{z_o e^{\gamma}} - 1] + \frac{u_*}{\kappa}\}]$$

$$= \frac{1}{a\kappa(u_* t)^2 t} [-2F - \eta \frac{\partial F}{\partial \eta} - \frac{\partial F}{\partial \beta} (\beta + \frac{1}{a\kappa} (\ell n \frac{\kappa u_* t}{z_o e^{\gamma}}))]$$

(2) $$\frac{\partial \chi}{\partial x} = \frac{1}{a\kappa(u_* t)^2} \frac{1}{au_* t} \frac{\partial F}{\partial \beta} = \frac{1}{a\kappa(u_* t)^2 t} [\frac{1}{au_*} \frac{\partial F}{\partial \beta}]$$

$$[\frac{u_*}{\kappa} \ell n \frac{z}{z_o}] \frac{\partial \chi}{\partial x} = \frac{1}{a\kappa(u_* t)^2 t} [\frac{1}{a\kappa} \ell n \frac{z}{z_o} \frac{\partial F}{\partial \beta}]$$

(3) $\frac{\partial}{\partial z}\left(\kappa u_* z \frac{\partial \chi}{\partial z}\right)$

$$\frac{\partial \chi}{\partial z} = \frac{\partial \chi}{\partial \eta}\frac{\partial \eta}{\partial z} = \frac{1}{a\kappa^2 (u_* t)^3}\frac{\partial F}{\partial \eta}$$

$$\frac{\partial}{\partial z}\left(\frac{\kappa u_* z}{a\kappa^2 (u_* t)^3}\frac{\partial F}{\partial \eta}\right) = \frac{1}{a u_* t^2}\cdot\frac{1}{\kappa u_* t}\frac{\partial}{\partial \eta}\left[\eta \frac{\partial F}{\partial \eta}\right] = \frac{1}{a\kappa (u_* t)^2 t}\left[\eta \frac{\partial^2 F}{\partial \eta^2} + \frac{\partial F}{\partial \eta}\right]$$

Substituting (1), (2) and (3) into equation (3.18) it can be shown that

$$\frac{1}{a\kappa (u_* t)^2 t}\left[\frac{\partial^2 F}{\partial \eta^2} + (\eta+1)\frac{\partial F}{\partial \eta} + \left[\beta - \frac{1}{a\kappa}\left(\ell n \frac{z}{z_o} - \ell n \frac{\kappa u_* t}{z_o e^\gamma}\right)\right] + 2F\right] = 0$$

$$\eta \frac{\partial^2 F}{\partial \eta^2} + (\eta+1)\frac{\partial F}{\partial \eta} + \left(\beta - \frac{1}{a\kappa}\ell n\, \eta e^\gamma\right)\frac{\partial F}{\partial \beta} + 2F = 0 \qquad (3.27)$$

Derivation of Equation (3.33b)

Consider the dispersion integral equation (3.33a):

$$\eta \frac{d^2\theta_2}{d\eta^2} + (\eta+1)\frac{d\theta_2}{d\eta} - \theta_2 = \frac{-2}{a^2\kappa^2}\ell n\, \eta e^\gamma \left[e^{-\eta}(\ell n\, \eta + \gamma - 1) + E_1(\eta)\right] \qquad (3.33a)$$

Multiplying the above equation by $(\eta+1)e^\eta$ and integrating it, the following results are obtained. First consider the integral of the left hand side of the above equation:

$$\int_o^\eta (\eta+1)\, e^\eta \left[\frac{d^2\theta_2}{d\eta^2} + (\eta+1)\frac{d\theta_2}{d\eta} - \theta_2\right] d\eta$$

$$= \eta e^\eta \left[(\eta+1)\frac{d\theta_2}{d\eta} - \theta_2\right]$$

<u>Check</u>

$$\frac{d}{d\eta}\left[\eta e^{\eta}\left((\eta+1)\frac{d\theta_2}{d\eta}-\theta_2\right)\right]$$

$$= \eta e^{\eta}\left[(\eta+1)\frac{d^2\theta_2}{d\eta^2}+\frac{d\theta_2}{d\eta}-\frac{d\theta_2}{d\eta}\right]$$

$$+ (\eta+1)\, e^{\eta}\left[(\eta+1)\frac{d\theta_2}{d\eta}-\theta_2\right]$$

$$= (\eta+1)\, e^{\eta}\left[\eta\frac{d^2\theta_2}{d\eta^2}+(\eta+1)\frac{d\theta_2}{d\eta}-\theta_2\right]$$

writing $\ell = \ell n\,(\eta e^{\gamma})$, (3.33a) can now be written as

$$\eta e^{\eta}\left[(\eta+1)\frac{d\theta_2}{d\eta}-\theta_2\right] = \frac{-2}{a^2\kappa^2}\int_0^{\eta}(\eta+1)\, e^{\eta}\,\ell\,\left[e^{-\eta}(\ell n\,\eta+\gamma-1)+E_1(\eta)\right]d\eta$$

$$= \frac{-2}{a^2\kappa^2}\left[\underset{(a)}{\int_0^{\eta}(\eta+1)e^{\eta}\,\ell\,E_1(\eta)d\eta} + \underset{(b)}{(\gamma-1)\int_0^{\eta}(\eta+1)e^{\eta}\,\ell\,d\eta} + \underset{(c)}{\int_0^{\eta}(\eta+1)\,\ell\,\ell n\,\eta\,d\eta}\right]$$

The integrals (a), (b), and (c) are performed as follows:

$$(a)\quad \int_0^{\eta}(\eta+1)\, e^{\eta}\,\ell\,E_1(\eta)d\eta = \int_0^{\eta}\eta e^{\eta}\,\ell\,E_1(\eta)d\eta + \int_0^{\eta}e^{\eta}\,\ell\,E_1(\eta)d\eta$$

$$= -\,\eta(1-\ell)e^{\eta}\,E_1(\eta) + \int_0^{\eta}\ell\,d\eta + \int_0^{\eta}\eta e^{\eta}\,E_1(\eta)d$$

$$= -\,\eta(1-\ell)e^{\eta}\,E_1(\eta) + \eta(\ell-1) + (e^{\eta}(\eta-1)E_1(\eta) + \eta - \ell)$$

$$= e^{\eta}\,E_1(\eta)\,(\eta\ell-1) + \eta\,\ell - \eta - \ell$$

(b) $$(\gamma-1)\int_0^\eta (\eta+1)\,\ell\,d\eta = (\gamma-1)\left[\int_0^\eta \eta\,\ell\,d\eta + \int_0^\eta \ell\,d\eta\right]$$

$$= (\gamma-1)\left[\frac{\eta^2}{2}(\ell-\frac{1}{2}) - \eta(1-\ell)\right]$$

(c) $$\int_0^\eta (\eta+1)\,\ell\,\ell n\,\eta\,d\eta$$

$$= \int_0^\eta \eta\,\ell\,\ell n\,\eta\,d\eta + \int_0^\eta \ell(\ell-\gamma)\,d\eta$$

$$= \frac{1}{2}\,[\eta^2\,\ell\,(-1+\ell n\,\eta) + \frac{\eta^2}{2}(\gamma+1)] + [\eta\ell^2-\gamma\eta(\ell-1) - 2\eta(\ell-1)]$$

Adding (a), (b) and (c) it can be shown that:

$$\eta e^\eta\left[(\eta+1)\frac{d\theta_2}{d\eta} - \theta_2\right] = \frac{-2}{a^2\kappa^2}\left[(e^\eta E_1(\eta) + \ell)(\eta\ell-1) + \eta^2\frac{(\ell-1)^2}{2} - 2\eta(\ell-1)\right]$$

$$(\eta+1)\frac{d\theta_2}{d\eta} - \theta_2 = \frac{-2}{a^2\kappa^2}\left[\frac{E_1(\eta)+\ell\,e^{-\eta}}{\eta}(\eta\ell-1) + \eta e^{-\eta}\frac{(\ell-1)^2}{2} - 2e^{-\eta}(\ell-1)\right]$$

Derivation of Equation (3.33c)

Consider the equation (3.33b):

$$(\eta+1)\frac{d\theta_2}{d\eta} - \theta_2 = -\frac{2}{a^2\kappa^2}\left[\frac{(E_1(\eta)+\ell\,e^{-\eta})}{\eta}(\eta\ell-1) + \eta\frac{e^{-\eta}(\ell-1)^2}{2} - 2e^{-\eta}(\ell-1)\right]$$

Writing the above equation as

$$(\eta+1)\frac{d\theta_2}{d\eta} - \theta_2 = G(\eta)$$

$$\frac{\theta_2}{\eta+1} = \frac{d\theta_2}{d\eta} - \frac{G(\eta)}{(\eta+1)} = \Phi(\eta) \qquad \text{(call)}$$

it can be shown that

$$\theta_2 = (\eta+1)\,\Phi(\eta)$$

and

$$\frac{d\theta_2}{d\eta} = \theta_2' = (\eta+1)\ \Phi' + \Phi$$

therefore,

$$\Phi' = (\theta_2' - \Phi)/(\eta+1) = G(\eta)/(\eta+1)^2$$

Integrating the equation for Φ' as shown below,

$$\int_\eta^\infty \Phi' d\eta = \int_\eta^\infty G(\eta)/(\eta+1)^2\ d\eta$$

$$\Phi \Big|_\eta^\infty = \int_\eta^\infty G(\eta)/(\eta+1)^2\ d\eta$$

where $\Phi = \dfrac{\theta_2}{\eta+1}$, and $\theta_2(\infty) = 0$.

It is obtained that

$$\theta_2(\eta) = -\ (\eta+1) \int_\eta^\infty G(\eta)/(\eta+1)^2\ d\eta$$

<u>Derivation of Equation (3.34)</u>

Consider equation (3.33c):

$$\theta_2(\eta) = \frac{2(\eta+1)}{a^2\kappa^2} \int_\eta^\infty \left[\frac{(E_1(\eta)+\ell\ e^{-\eta}}{\eta(\eta+1)^2} (\eta\ell-1) + \frac{\eta e^{-\eta}(\ell-1)^2}{2(\eta+1)^2} - \frac{2e^{-\eta}(\ell-1)}{(\eta+1)^2} \right] d\eta \tag{3.33c}$$

Recall that $E_1(\eta) = \int_\eta^\infty \dfrac{e^{-\eta}}{\eta}\ d\eta$ and $\ell = \ell n\ (\eta e^\gamma)$;

The integration in (3.33c) is performed term by term as shown below:

(a) $$\int_\eta^\infty \frac{E_1(\eta)\ell}{(\eta+1)^2}\ d = \frac{E_1(\eta)\ell}{\eta+1} + \int_\eta^\infty \frac{E_1(\eta) - e^{-\eta}\ell}{\eta(\eta+1)}\ d\eta$$

(b) $$-\int \frac{E_1(\eta)}{\eta(\eta+1)^2}\ d\eta = -\int \frac{E_1(\eta)}{\eta(\eta+1)}\ d\eta + \int \frac{E_1(\eta)}{(\eta+1)^2}\ d\eta$$

(c) $\int \frac{\ell^2 e^{-\eta}}{(\eta+1)^2} d\eta$

(d) $-\int \frac{\ell e^{-\eta}}{\eta(\eta+1)^2} d\eta = -\int \frac{\ell e^{-\eta}}{\eta(\eta+1)} d\eta + \int \frac{\ell e^{-\eta}}{(\eta+1)^2} d\eta$

(e) $\int \frac{\eta e^{-\eta} \ell^2}{2(\eta+1)^2} d\eta = \frac{e^{-\eta}}{2(\eta+1)} \ell^2 - \int \frac{e^{-\eta} \ell^2}{(\eta+1)^2} d\eta + \int \frac{e^{-\eta}\ell}{\eta(\eta+1)} d\eta$

(f) $-\int \frac{\eta e^{-\eta}\ell}{(\eta+1)^2} d\eta = -\frac{e^{-\eta}}{\eta+1} \ell - \int \frac{e^{-\eta}}{\eta(\eta+1)} d\eta + 2\int \frac{e^{-\eta} \ell}{(\eta+1)^2} d\eta$

(g) $\int \frac{\eta e^{-\eta}}{\eta(\eta+1)^2} d\eta = -\frac{e^{-\eta}}{2(\eta+1)} - \int \frac{e^{-\eta}}{(\eta+1)^2} d\eta$

(h) $-\int 2 \frac{e^{-\eta} \ell}{(\eta+1)^2} d\eta$

(i) $2\int \frac{e^{-\eta}}{(\eta+1)^2} d\eta$

Substituting these results in (3.33c) it can be written that,

$$\theta_2(\eta) = \frac{2(\eta+1)}{a^2\kappa^2} \left[\int_\eta^\infty \left[\frac{\ell e^{-\eta}}{(\eta+1)^2} - \frac{\ell e^{-\eta}}{\eta(\eta+1)} - \frac{e^{-\eta}}{\eta(\eta+1)} + \frac{E_1(\eta)}{(\eta+1)^2} + \frac{e^{-\eta}}{(\eta+1)^2}\right] d\eta \right.$$

$$\left. + \frac{1}{(\eta+1)} \left(\frac{e^{-\eta} \ell^2}{2} + E_1(\eta)\ell - e^{-\eta}\ell + e^{-\eta}/2\right) \right]$$

The integrations in the above equation are performed as shown below:

(1) $\int_\eta^\infty \frac{\ell e^{-\eta}}{(\eta+1)^2} d\eta = \frac{\ell e^{-\eta}}{\eta+1} + \int_\eta^\infty \frac{e^{-\eta}}{\eta(\eta+1)} d\eta - \int \frac{e^{-\eta}\ell}{(\eta+1)} d\eta$

$$(2) \quad -\int_{\eta}^{\infty} \frac{e^{-\eta}\,\ell}{\eta(\eta+1)}\,d\eta = -\int \frac{e^{-\eta}}{\eta}\,\ell\,d\eta + \int \frac{e^{-\eta}\,\ell}{(\eta+1)}\,d\eta$$

$$(3) \quad \int_{\eta}^{\infty} \frac{E_1(\eta)}{(\eta+1)^2}\,d\eta = \frac{E_1(\eta)}{(\eta+1)} - \int_{\eta}^{\infty} \frac{e^{-\eta}}{\eta(\eta+1)}\,d\eta$$

$$= \frac{E_1(\eta)}{(\eta+1)} - E_1(\eta) + \int \frac{e^{-\eta}}{(\eta+1)}\,d\eta$$

$$(4) \quad \int_{\eta}^{\infty} \frac{e^{-\eta}}{(\eta+1)^2}\,d\eta = \frac{e^{-\eta}}{\eta+1} - \int \frac{e^{-\eta}}{\eta+1}\,d\eta$$

Substituting these results in the equation for $\theta_2(\eta)$, it can be written as

$$\theta_2(\eta) = \frac{1}{a^2\kappa^2}\,[2\,E_1(\eta)\ell + e^{-\eta}\ell^2 + 3e^{-\eta} - 2\eta E_1(\eta) - \frac{1}{2(\eta+1)} \int_{\eta}^{\infty} \frac{e^{-\eta}}{\eta}\,\ell\,d\eta$$

The last integral in the previous equation can now be written as

$$-\int \frac{e^{-\eta}\,\ell}{\eta}\,d\eta = -\frac{e^{-\eta}\,\ell^2}{2}\Big|_{\eta}^{\infty} - \int_{\eta}^{\infty} \frac{e^{-\eta}\ell n^2\,(\eta e^{\gamma})}{2}\,d\eta$$

$$= \frac{e^{-\eta}\,\ell^2}{2} - \frac{1}{2}\left[\int_{\eta}^{\infty} e^{-\eta}\ell n^2\,\eta\,d\eta + 2\,\gamma \int_{\eta}^{\infty} e^{-\eta}\,\ell n\,\eta\,d\eta + \gamma^2\right]$$

$$= \frac{e^{-\eta}\,\ell^2}{2} - \frac{1}{2}\left[\Gamma''(1,\eta) + 2\,\gamma\,\Gamma'\,(1,\eta) + \gamma^2\right]$$

where $\Gamma^{n}\,(a,\eta) = \partial^{n}\,\Gamma(a,\eta) = \int_{\eta}^{\infty} e^{-t}\,t^{a-1}\,(\ell n\,t)^{n}\,dt$ are the derivatives of incomplete gamma function. It can now be written,

$$\theta_2(\eta) = \frac{1}{a^2\kappa^2}\left\{2\,E_1(\eta)\ell + \ell^2\,e^{-\eta}\,(\eta+2) - 2\eta\,E_1(\eta) + 3e^{-\eta} - (\eta+1)\left[\Gamma''(1,\eta) + 2\gamma\,\Gamma'(1,\eta) + \gamma^2 e^{-\eta}\right]\right\}$$

Asymptotic Properties of $\theta_2(\eta)$

Consider equation (3.34):

$$\theta_2(\eta) = \frac{1}{a^2\kappa^2}\left\{2E_1(\eta)\ell + \ell^2 e^{-\eta}(\eta+2) - 2\eta E_1(\eta) + 3e^{-\eta} - (\eta+1)\left[\Gamma''(1,\eta) + 2\gamma\Gamma'(1,\eta) + \gamma^2 e^{-\eta}\right]\right\}$$

$$= \frac{1}{a^2\kappa^2}\left\{2\ell\,[E_1(\eta) + \ell e^{-\eta}] + \eta[\ell^2 e^{-\eta} - 2E_1(\eta)] + 3e^{-\eta} - (\eta+1)\,[\Gamma''(1,\eta) + 2\gamma\Gamma'(1,\eta) + \gamma^2 e^{-\eta}]\right\} \qquad (3.34)$$

Noting the following asymptotic properties ,

$$\lim_{\eta\to o}\ [E_1(\eta) + \ell\, e^{-\eta}] \to 0$$

$$\lim_{\eta\to o}\ \Gamma''(1,\eta) \to \frac{\pi^2}{6} + \gamma^2$$

$$\lim_{\eta\to o}\ \Gamma'(1,\eta) \to -\gamma$$

$$\lim_{\eta\to\infty}\ \eta\, E_1(\eta) \to 0$$

it can be shown that,

$$\lim_{\eta\to o}\ \theta_2(\eta) = \frac{1}{a^2\kappa^2}(3 - \pi^2/6)$$

and

$$\lim_{\eta\to\infty}\ \theta_2(\eta) \to 0 .$$

Derivation of $\int_0^\infty \theta_2(\eta)\, d\eta$

Rearranging the terms in (3.34) it can be written that,

$$\int_0^\infty \theta_2(\eta)d\eta = \frac{1}{a^2\kappa^2} \int_0^\infty \Big\{ \underbrace{2\,\ell[E_1(\eta) + e^{-\eta}(\ell-1)]}_{(a)} + \underbrace{2\ell e^{-\eta}}_{(b)} + \underbrace{\eta\,\ell^2 e^{-\eta}}_{(c)} \underbrace{-2\eta E_1(\eta)}_{(d)}$$

$$+ \underbrace{3e^{-\eta}}_{(e)} - \underbrace{(\eta+1)\int_\eta^\infty e^{-\eta}\,\ell^2\, d\eta}_{(f)} \Big\}\, d\eta$$

Integrations in the above equation are performed as shown below:

(a) $\displaystyle\int_0^\infty 2\,\ell\,[E_1(\eta) + e^{-\eta}(\ell-1)]d\eta$

$$= \int_0^\infty 2\,\ell n\,\eta[e^{-\eta}(\ell n\,\eta + \gamma - 1) + E_1(\eta)]d\eta + 2\gamma \underbrace{\int_0^\infty [e^{-\eta}(\ell-1) + E_1(\eta)]d\eta}_{\equiv\, 0}$$

$$= 2(\frac{\pi^2}{6} + \gamma^2) - 2\gamma(\gamma-1) - 2(\gamma+1) = 2\,(\frac{\pi^2}{6} - 1)$$

(b) $\displaystyle\int_0^\infty 2\,\ell\, e^{-\eta}\, d\eta = 2(-\gamma+\gamma) = 0$

(c) $\displaystyle\int_0^\infty \eta\,\ell^2\, e^{-\eta}\, d\eta = (-2\gamma+\gamma^2 + \frac{\pi^2}{6} + 2\gamma(1-\gamma) + \gamma) = \frac{\pi^2}{6}$

(d) $\displaystyle -\int_0^\infty 2\eta\, E_1(\eta)\, d\eta = -\,\eta^2\, E_1(\eta)\,\Big|_0^\infty - \int_0^\infty \eta\, e^{-\eta}\, d\eta = -\,1$

(e) $\displaystyle\int 3e^{-\eta}\, d\eta = 3$

(f) $$-\int_0^\infty [(\eta+1) \int_\eta^\infty e^{-\eta}\, \ell^2\, d\eta]d\eta$$

$$= -\frac{(\eta+1)^2}{2} \int_\eta^\infty e^{-\eta}\, \ell^2\, d\eta \Big|_0^\infty - \int_0^\infty \frac{(\eta+1)^2}{2}\, e^{-\eta}\, \ell^2\, d\eta$$

$$= \frac{1}{2}(\pi^2/6) - \int_0^\infty \frac{\eta^2}{2} e^{-\eta}\, \ell^2\, d\eta - \int_0^\infty \eta\, e^{-\eta}\, \ell^2\, d\eta - \frac{1}{2}\int_0^\infty e^{-\eta}\, \ell^2\, d\eta$$

$$= \frac{1}{2}(\pi^2/6) - (\frac{\pi^2}{6} + 1) - \pi^2/6 - \frac{1}{2}(\pi^2/6) = -1 - 2\,\pi^2/6$$

Substituting these results into the integral for $\theta_2(\eta)$ it can be shown that,

$$\int_0^\infty \theta_2(\eta)d\eta = \frac{1}{a^2\kappa^2}\left\{2\,(\frac{\pi^2}{6} - 1) + \frac{\pi^2}{6} - 1 + 3 - (2\,\frac{\pi^2}{6} + 1)\right\}$$

$$= \frac{1}{a^2\kappa^2}(\frac{\pi^2}{6} - 1)$$

Derivation of Equation (3.38)

Consider equation (3.30d) for the third moment:

$$\eta\,\frac{d^2\theta_3}{d\eta^2} + (\eta+1)\frac{d\theta_3}{d\eta} - 2\theta_3 = -\frac{3\theta_2}{a^3\kappa^3}\,\ell \tag{3.30d}$$

Multiplying the above equation by $(\eta^2 + 4\eta + 2)e^\eta$ and integrating we obtain:

$$\int_0^\eta (\eta^2+4\eta+2)e^\eta[\eta\,\frac{d^2\theta_3}{d\eta^2} + (\eta+1)\frac{d\theta_3}{d\eta} - 2\theta_3]d\eta = \frac{-3}{a^3\kappa^3}\int_0^\eta (\eta^2+4\eta+2)e^\eta\theta_2\,\ell\,d\eta$$

Integration of L.H.S. of the above equation gives

$$\eta e^\eta[(\eta^2+4\eta+2)\frac{d\theta_3}{d\eta} - 2(\eta+2)\,\theta_3]$$

Check: Differentiating the result we get back the integrand

$$\frac{d}{d\eta}\left\{\eta e^{\eta}\left[(\eta^2+4\eta+2)\frac{d\theta_3}{d\eta} - 2(\eta+2)\theta_3\right]\right\}$$

$$= (\eta+1)e \quad \left[(\eta^2+4\eta+2)\frac{d\theta_3}{d\eta} - 2\ (\eta+2)\theta_3\right]$$

$$+ \ \eta e^{\eta}\left((\eta^2+4\eta+2)\frac{d^2\theta_3}{d\eta^2} + 2(\eta+2)\frac{d\theta_3}{d\eta} - 2(\eta+2)\frac{d\theta_3}{d\eta} - 2\theta_3\right)$$

$$= e^{\eta}(\eta^2+4\ \ +2)\left[\eta\frac{d^2\theta_3}{d\eta^2} + (\eta+1)\frac{d\theta_3}{d\eta} - 2\theta_3\right]$$

Therefore, it can be written

$$(\eta^2+4\eta+2)\frac{d\theta_3}{d\eta} - 2(\eta+2)\theta_3 = -\frac{3}{a^3\kappa^3}\ \frac{e^{-\eta}}{\eta}\int_0^{\eta}(\eta^2+4\eta+2)e^{\eta}\theta_2\ \ell dy$$

Derivation of Equation (3.41)

Consider equation (3.30d):

$$\underset{(1)}{\eta\frac{d^2\theta_3}{d\eta^2}} + \underset{(2)}{(\eta+1)\frac{d\theta_3}{d\eta}} - \underset{(3)}{2\theta_3} = -\frac{\theta_2}{a^3\kappa^3}\ \ell n\ \eta e^{\gamma} \qquad (3.30d)$$

Integrating the above equation from $\eta = 0$ to ∞ using the boundary conditions, the following results are obtained:

$$\left.\begin{array}{lll} \eta^{n}\ \theta_3(n) \to 0 & \text{as} & \eta \to \infty \\ \eta^{n}\dfrac{d\theta_3}{d\eta} \to 0 & \text{as} & \eta \to \infty \\ \eta\dfrac{d\theta_3}{d\eta} \to 0 & \text{as} & \eta \to 0 \end{array}\right\} \quad \text{Boundary conditions}$$

$$(1)\quad \int_0^{\infty}\eta\frac{d^2\theta_3}{d\eta^2}\,d\eta = \eta\cancelto{0}{\frac{d\theta_3}{d\eta}}\Bigg|_0^{\infty} - \int_0^{\infty}\frac{d\theta_3}{d\eta}\,d\eta$$

$$= -\ \theta_3\Big|_0^{\infty} = \theta_3(0)$$

$$(2) \quad \int_0^\infty (\eta+1) \frac{d\theta_3}{d\eta} \, d\eta = (\eta+1)\, \theta_3 \Big|_0^\infty - \int_0^\infty \theta_3 d\eta$$

$$= -\theta_3(0) - \int_0^\infty \theta_3 d\eta$$

$$(3) \quad -\int_0^\infty 2\theta_3 \, d\eta$$

Substituting (1), (2) & (3) into the eq. (3.30d) we get,

$$-3 \int_0^\infty \theta_3 d\eta = -\frac{3}{a^3\kappa^3} \int_0^\infty \theta_2 \, \ell n \;\; \eta e^\gamma \, d\eta$$

Therefore, it can be shown that,

$$\int_0^\infty \theta_3 \, d\eta = \frac{1}{a^3\kappa^3} \int_0^\infty \theta_2 \;\; \ell n \; \eta e^\gamma \, d\eta \quad .$$

Consider the integral on the R.H.S. of the previous equation

$$\int_0^\infty \theta_2 \, \ell n \, (\eta e^\gamma) \, d\eta$$

$$= \int_0^\infty [\underset{(a)}{2\, E_1(\eta)\, \ell} + \underset{(b)}{\ell^2\, e^{-\eta}(\eta+2)} - \underset{(c)\ (d)}{2\eta\, E_1(\eta)} + \underset{(e)}{3\, e^{-\eta}} - \underset{(f)}{(\eta+1) \int_\eta^\infty e^{-\eta}\, \ell^2 \, d\eta}]\ell \, d\eta$$

The integrations in the above equation are performed term by term as shown below:

$$(a) \quad \int_0^\infty 2\, \ell^2 \, E_1(\eta)\, d\eta = \int_0^\infty 2\, (\ell n^2\, \eta + 2\gamma\, \ell n\, \eta + \gamma^2)\, E_1(\eta)\, d\eta$$

$$= 2\, [(\frac{\pi^2}{6} + \gamma^2 + 2\gamma + 2) - 2\gamma(\gamma+1) + \gamma^2] = 4 + 2\,\frac{\pi^2}{6}$$

(b) $$\int_0^\infty 2\,\ell^3 e^{-\eta} d\eta = 2\int_0^\infty (\ell n^3\,\eta + 3\gamma\,\ell n^2\,\eta + 3\,\gamma^2\,\ell n\,\eta + \gamma^3)\,e^{-\eta}\,d\eta$$

$$= 2\,(-\gamma^3 - 3\gamma\,\frac{\pi^2}{6} - 2\sum_{m=0}^{\infty}\frac{1}{(1+m)^3}) + 6\gamma\,(\frac{\pi^2}{6} + \gamma^2) -$$

$$6\,\gamma^3 + 2\gamma^3 = -4\sum_{m=0}^{\infty}\frac{1}{(1+m)^3}$$

(c) $$\int_0^\infty \eta\,\ell^3\,e^{-\eta}\,d\eta = -\,(\eta+1)\,e^{-\eta}\,\ell^3\Big|_0^\infty + \int_0^\infty (\eta+1)\,e^{-\eta}\,\frac{3\ell^2}{\eta}\,d\eta$$

$$= -\,(\eta+1)\,e^{-\eta}\,\ell^3\Big|_0^\infty + \int_0^\infty 3e^{-\eta}\,\ell^2\,d\eta + e^{-\eta}\,\ell^3\Big|_0^\infty +$$

$$\int_0^\infty e^{-\eta}\,\ell^3\,d\eta$$

$$= -\,\eta e^{-\eta}\,\ell^3\Big|_0^\infty + \int_0^\infty 3\,e^{-\eta}\,\ell^3\,d\eta + \int_0^\infty e^{-\eta}\,\ell^3\,d\eta$$

$$= \frac{3\pi^2}{6} + [(-\gamma^3 + 3\gamma\,\frac{\pi^2}{6} - 2\sum_{m=0}^{\infty}\frac{1}{(1+m)^3}) + 3\gamma\,(\frac{\pi^2}{6} + \gamma^2) - 3\gamma^3 + \gamma^3]$$

$$= 3\,\frac{\pi^2}{6} - 2\sum_{m=0}^{\infty}\frac{1}{(1+m)^3}$$

(d) $$-\int_0^\infty 2\eta\,\ell\,E_1(\eta)\,d\eta = -\,2\,[\int_0^\infty \eta\,\ell n\,\eta\,E_1(\eta)\,d\eta + \gamma\int_0^\infty \eta\,E_1(\eta)\,d\eta]$$

$$= -\,2\,[\frac{\eta^2}{2}\,\ell n\,\eta\,E_1(\eta)\Big|_0^\infty - \int_0^\infty \frac{\eta^2}{2}\,(\frac{E_1(\eta)}{\eta} - \frac{e^{-\eta}}{\eta}\,\ell n\,\eta)\,d\eta + \gamma/2]$$

$$= -\,2\,[-\,\frac{1}{4} + (1-\gamma)/2 + \gamma/2] = -\,1/2$$

(e) $\int_0^\infty 3e^{-\eta}\,\ell\,d\eta \equiv 0$

(f) $\int_0^\infty -\,(\eta+1)\,\ell\,[\int_\eta^\infty e^{-\eta}\,\ell^2\,d\eta]\,d\eta$

$$= -\int_0^\infty \eta\,\ell\,(\int_\eta^\infty e^{-\eta}\,\ell^2\,d\eta]\,d\eta - \int_0^\infty \ell\,(\int_\eta^\infty e^{-\eta}\,\ell^2\,d\eta)d\eta$$

$$= -\,[\frac{\eta^2}{2}\,(\ell-\frac{1}{2})\int_\eta^\infty e^{-\eta}\,\ell^2\,d\eta\,\Big|_0^\infty + \int_0^\infty \frac{\eta^2}{2}\,(\ell-\frac{1}{2})\,e^{-\eta}\,\ell^2\,d\eta$$

$$+\,\eta(\ell-1)\int_\eta^\infty e^{-\eta}\,\ell^2\,d\eta\,\Big|_0^\infty + \int_0^\infty \eta\,(\ell-1)\,e^{-\eta}\,\ell^2\,d\eta$$

$$= -\,[\int_0^\infty \frac{\eta^2}{2}\,\ell^3\,e^{-\eta}\,d\eta - \int_0^\infty \frac{\eta^2}{2}\,e^{-\eta}\,\ell^2\,d\eta + \int_0^\infty \eta\,\ell^3\,e^{-\eta}\,d\eta -$$

$$\int_0^\infty \eta\,\ell^2\,e^{-\eta}\,d\eta]$$

$$= -\,[(\frac{9}{2}\cdot\frac{\pi^2}{6} - 2\sum_{m=0}^\infty \frac{1}{(1+m)^3}) - \frac{1}{2}\,(\frac{\pi^2}{6}+1) + (3\,\frac{\pi^2}{6} - 2\sum_{m=0}^\infty \frac{1}{(1+m)^3}) - \frac{\pi^2}{6}$$

$$= -\,[\pi^2 - 4\sum_{m=0}^\infty \frac{1}{(1+m)^3} - \frac{1}{2}] - [3\,\frac{\pi^2}{6} - 2\sum_{m=0}^\infty \frac{1}{(1+m)^3} - \frac{\pi^2}{6}]$$

$$= -\,[\pi^2 - 4\sum_{m=0}^\infty \frac{1}{(1+m)^3} - \frac{1}{2}]$$

Note:

$$\int_0^\infty \eta^2\,e^{-\eta}\,\ell^3\,d\eta = 9\,\frac{\pi^2}{6} - 4\sum_{m=0}^\infty \frac{1}{(1+m)^3}$$

Therefore, it can be shown that

$$\int_0^\infty \theta_3 \, d\eta = \frac{1}{a^3\kappa^3} [(a) + (b) + (c) + (d) + (e) + (f)]$$

$$= \frac{1}{a^3\kappa^3} [4 - \frac{\pi^2}{6} - 2 \sum_{m=0}^{\infty} \frac{1}{(1+m)^3}]$$

The term under the summation is given by Euler's 'ψ' function (tabulated)

$$\psi''(1) = - 2 \sum_{m=0}^{\infty} \frac{1}{(1+m)^3} \simeq -2.404$$

Therefore, it can be written

$$\int_0^\infty \theta_3 \, d\eta = \frac{1}{a^3\kappa^3} [4 - \frac{\pi^2}{6} + \psi''(1)]$$

Multiplying the equation (3.30d) by η , it is integrated as shown:

$$\int_0^\infty [\underset{(a)}{\eta^2 \frac{d^2\theta_3}{d\eta^3}} + \underset{(b)}{\eta(\eta+1) \frac{d\theta_3}{d\eta}} - \underset{(c)}{2\eta\theta_3}]d\eta = - \frac{3}{a^3\kappa^3} \int_0^\infty \theta_2 \, \eta \, \ell \, d\eta$$

The above integration is performed term by term by using the boundary conditions, as shown below:

$$(a) \quad \int_0^\infty \eta^2 \frac{d^2\theta_3}{d\eta^2} d\eta = \eta^2 \frac{d\theta_3}{d\eta} \Big|_0^\infty - \int_0^\infty 2\eta \frac{d\theta_3}{d\eta} d\eta$$

$$= - 2\eta\theta_3 \Big|_0^\infty + \int_0^\infty 2 \, \theta_3 \, d\eta$$

$$\text{(b)} \quad \int_0^\infty (\eta^2+\eta) \frac{d\theta_3}{d\eta} \; d\eta = (\eta^2+\eta)\; \theta_3 \Big|_0^\infty - \int_0^\infty (2\eta+1)\; \theta_3 \; d\eta$$

$$= - \int_0^\infty 2\eta\theta_3 \; d\eta - \int_0^\infty \theta_3 d\eta$$

$$\text{(c)} \quad - \int_0^\infty 2\eta\theta_3 \; d\eta \; .$$

Substituting the results in (a), (b) & (c) into the above equation it can be shown

$$\int_0^\infty \eta \; \theta_3 d\eta = \frac{1}{4} \; [\int_0^\infty \theta_3 \; d\eta + \frac{3}{a^3 \kappa^3} \int_0^\infty \theta_2 \; \eta \; \ell \; d\eta]$$

Now, consider the integral $\int_0^\infty \theta_2 \eta \ell d\eta$,

Substituting (3.34) for θ_2 , it can be shown

$$\int_0^\infty \eta \; \ell \; [\underset{\text{(a)}}{2 \; E_1(\eta) \; \ell} + \underset{\text{(b)}}{\ell^2 \; e^{-\eta}}\underset{\text{(c)}}{(\eta+2)} - \underset{\text{(d)}}{2\eta E_1(\eta)} + \underset{\text{(e)}}{3e^{-\eta}} - \underset{\text{(f)}}{(\eta+1) \int_\eta^\infty e^{-\eta} \; \ell^2 \; d\eta}]d\eta$$

The above integration is performed term by term as shown below:

$$\text{(a)} \quad \int_0^\infty 2\eta \; \ell^2 \; E_1(\eta) \; d\eta = \eta^2 \; (\ell - \frac{1}{2}) \; E_1(\eta) \Big|_0^\infty + 2 \int_0^\infty (\frac{\eta\ell^2}{2} \; e^{-\eta} - \eta \; \frac{e^{-\eta}\ell}{4}) \; d\eta$$

$$= \frac{\pi^2}{6} - \frac{1}{2} \; (1-\gamma+\gamma) = \frac{\pi^2}{6} - \frac{1}{2}$$

$$\text{(b)} \quad \int_0^\infty \eta^2 \; \ell^3 \; e^{-\eta} \; d\eta = 9 \; \frac{\pi^2}{6} - 4 \sum_{m=0}^\infty \frac{1}{(1+m)^3}$$

(c) $\int_0^\infty 2\eta^3 e^{-\eta}\, d\eta = 6\,\frac{\pi^2}{6} - 4 \sum_{m=0}^{\infty} \frac{1}{(1+m)^3}$

(d) $-\int_0^\infty 2\,\eta^2\,\ell^2\, E_1(\eta)\, d\eta = -\left[2\,E_1(\eta)\,\frac{\eta^3}{3}(\ell - \frac{1}{3})\right]\Big|_0^\infty + 2\int_0^\infty \frac{\eta^2}{3}\,(\ell - \frac{1}{3})e^{-\eta}d\eta]$

$$= -2\,[\frac{1}{3}\,(3 - 2\gamma + 2\gamma - \frac{2}{3})] = -14/9$$

(e) $\int_0^\infty 3\eta\,\ell\, e^{-\eta}\, d\eta = 3\,(1-\gamma+\gamma) = 3$

(f) $-\int_0^\infty \eta(\eta+1)\,\ell\,\left(\int_\eta^\infty e^{-\eta}\,\ell^2\, d\eta\right) d\eta$

$$= \underbrace{-\int_0^\infty \eta^2\,\ell\,\left(\int_\eta^\infty e^{-\eta}\,\ell^2\, d\eta\right) d\eta}_{(1)} \underbrace{- \int_0^\infty \eta\,\ell\,\left(\int_\eta^\infty e^{-\eta}\,\ell^2\, d\eta\right) d\eta}_{(2)}$$

(1) $= -\left[\frac{\eta^3}{3}\,(\ell - \frac{1}{3})\int_\eta^\infty e^{-\eta}\,\ell^2\, d\eta\right]\Big|_0^\infty + \int_0^\infty \frac{\eta^3}{3}\,(\ell - \frac{1}{3})\, e^{-\eta}\,\ell^2\, d\eta$

$$= -\int_0^\infty \frac{\eta^3}{3}\, e^{-\eta}\,\ell^3\, d\eta + \int_0^\infty \frac{\eta^3}{9}\, e^{-\eta}\,\ell^2\, d\eta$$

$$= -\frac{1}{3}\,[33\,\frac{\pi^2}{6} + 6 - 12\sum_{m=0}^{\infty}\frac{1}{(1+m)^3}] + \frac{1}{9}\,[9\,\frac{\pi^2}{6} - 4\sum_{m=0}^{\infty}\frac{1}{(1+m)^3}]$$

(2) $= -\int_0^\infty \eta\,\ell\,\left(\int_\eta^\infty e^{-\eta}\,\ell^2\, d\eta\right) d\eta$ (see page 67)

$$= - [4 \frac{\pi^2}{6} - \frac{1}{2} - 2 \sum_{m=0}^{\infty} \frac{1}{(1+m)^3}]$$

Therefore $\quad (f) = (1) + (2) = - [14 \frac{\pi^2}{6} + \frac{3}{2} - \frac{50}{9} \sum_{m=0}^{\infty} \frac{1}{(1+m)^3}]$

Substituting the results of (a), (b) .... (f) into the integral equation it can be shown that

$$\int_0^{\infty} \eta \, \theta_2 \, \ell \, d\eta = [2 \frac{\pi^2}{6} - \frac{5}{9} + \frac{11}{9} \psi''(1)]$$

$$\text{where} \quad \psi''(1) = -2 \sum_{m=0}^{\infty} \frac{1}{(1+m)^3} \simeq -2.404$$

Derivatives of Incomplete Gamma Functions

Gamma Function: $\Gamma(a,x) = \int_x^{\infty} e^{-t} \, t^{a-1} \, dt$

n^{th} derivative w·r·t parameter 'a' $= \dfrac{\partial^n \Gamma(a,x)}{\partial a^n} = \int_x^{\infty} e^{-t} \, (\ell n \, t)^n \, t^{a-1} \, dt$

$$\Gamma'(1,x) = \int_x^{\infty} e^{-t} \, \ell n \, t \, dt = \ell n \, x \, e^{-x} + E_1(x)$$

$$\Gamma'(2,x) = \int_x^{\infty} e^{-t} \, \ell n \, t \cdot t \, dt = e^{-x}(x \, \ell n \, x + 1) + \Gamma'(1,x)$$

$$\Gamma''(1,x) = \int_x^{\infty} e^{-t} \, (\ell n \, t)^2 \, dt$$

$$\Gamma''(2,x) = \int_x^{\infty} t \, e^{-t} \, (\ell n \, t)^2 \, dt$$

$$= \int_0^{\infty} t \, e^{-t} \, (\ell n \, t)^2 \, dt - \int_0^{x} t \, e^{-t} \, (\ell n \, t)^2 \, dt$$

$$= \frac{\pi^2}{6} + \gamma^2 - 2\gamma - \int_0^t t\ e^{-t}\ (\ell n\ t)^2\ dt$$

$$\Gamma''(2,x) = \int_x^\infty t\ e^{-t} (\ell n\ t)^2\ dt = -\ (t+1)\ e^{-t}\ (\ell n\ t)^2 \Big|_x^\infty + \int_x^\infty (t+1) e^{-t}\ 2\ \frac{\ell n\ t}{t}\ dt$$

$$= (x+1)\ e^{-x}\ (\ell n\ x)^2 + \int_x^\infty 2\ e^{-t}\ \ell n\ t\ dt + \int_x^\infty 2\ e^{-t}\ \frac{\ell n\ t}{t}\ dt$$

$$e^{-t}\ (\ell n\ t)^2 \Big|_x^\infty + \int_x^\infty e^{-t}\ (\ell n\ t)^2\ dt$$

$$= x\ e^{-x}\ (\ell n\ x)^2 + \int_x^\infty 2\ e^{-t}\ \ell n\ t\ dt + \int_x^\infty e^{-t}\ (\ell n\ t)^2\ dt$$

$$\Gamma''(2,x) = x\ e^{-x}\ (\ell n\ x)^2 + 2\ \Gamma'(1,x) + \Gamma''(1,x)$$

$$\Gamma''(1,x) = \int_x^\infty e^{-t}\ (\ell n\ t)^2\ dt = \Gamma''(2,x) - x\ e^{-x}\ (\ell n\ x)^2 - 2\Gamma'(1,x)$$

$$= \Gamma''(2,x) - e^{-x}\ \ell n\ x\ [x\ \ell n\ x + 2] - 2\ E_1(x)$$

Similarly the following derivatives can be derived,

$$\Gamma''(1,x) = e^{-x}\ (\ell n\ x)^2 + 2\Gamma'(o,x)\ :\ x = 0 \quad \Gamma''(1,0) = \frac{\pi^2}{6} + \gamma^2$$

$$\Gamma''(2,x) = x\ e^{-x}\ (\ell n\ x)^2 + 2\Gamma'(1,x) + \Gamma''(1,x)$$

$$\Gamma''(3,x) = x^2\ e^{-x}\ (\ell n\ x)^2 + 2\Gamma'(2,x) + 2\Gamma''(2,x)$$

$$\Gamma''(4,x) = x^3\ e^{-x}\ (\ell n\ x)^2 + 2\Gamma'(3,x) + 3\Gamma''(3,x)$$

$$\vdots$$

$$\Gamma''(n,x) = x^{n-1}\ e^{-x}\ (\ell n\ x)^2 + 2\Gamma'((n-1),x) + (n-1)\Gamma''((n-1),x)$$

$$\Gamma'(1,x) = e^{-x}\ \ell n\ x + E_1(x) \qquad x=0\ \Gamma'(1,0) = -x$$

$$\Gamma'(2,x) = x\, e^{-x}\, \ell n\, x + e^{-x} + \Gamma'(1,x)$$

$$\Gamma'(3,x) = x^2\, e^{-x}\, \ell n\, x + (x+1)\, e^{-x} + 2\Gamma'(2,x)$$

$$\Gamma'(4,x) = x^3\, e^{-x}\, \ell n\, x + (x^2 + 2x + 2)\, e^{-x} + 3\Gamma'(3,x)$$

$$\Gamma'(5,x) = x^4\, e^{-x}\, \ell n\, x + (x^3 + 3x^2 + 6x + 6)\, e^{-x} + 4\Gamma'(4,x)$$

$$\vdots$$

$$\Gamma'(n,x) = x^{n-1}\, e^{-x}\, \ell n\, x + (x^{n-2} + (n-2)\, x^{n-3} + (n-2)!(x^{n-4} + 1))$$

$$+ (n-1)\Gamma'(n-1,x)$$

APPENDIX II

QUASI-CONTINUOUS LINE SOURCE

COMPUTER PROGRAM

APPENDIX II

QUASICONTINUOUS LINE SOURCE

```
      DIMENSION E(2200),Q(120    ,P(320),X(120)
C     THIS PROGRAM CALCULATES THE CONCENTRATION FIELD DOWN
C     WIND OF A LINE SOURCE.  CONTAMINANTS ARE PASSIVE
C     AND ARE RELEASED FOR A FINITE TIME (20 SEC) AT GROUND
C     LEVEL.  ATMOSPHERE IS NEUTRALLY STABLE.  VELOCITY
C     DISTRIBUTION IS LOGRITHAMIC WITH U*=2.5 AND Z0=0.1 FT
C     CONCENTRATION FIELD IS OBTAINED, 10 SECONDS AFTER
C     RELEASE OF CONTAMINANTS.
      READ(5,3)(E(I),I=1,2079)
    3 FORMAT(7F11.9)
C     E(I) IS EXPONENTIAL INTEGRAL. (TABULATED).  IT READS
C     E(I) FOR I=0.001 TO 2.00 AND THEN I=2.1 TO 10.0 WITH
C     INTERVALS OF 0.001 AND 0.1 RESPECTIVELY.
      A=1.5
C     A=1.5 IS CONSTANT IN LONGITUDINAL VARIANCE
      B=0.4
      C=0.4
C     C=KARMAN CONSTANT
      USTAR=2.5
C     USTAR= SHEAR VELOCITY
      Z0=0.1
C     Z0= ROUGHNESS COEFFICIENT
      GM=0.5772156649
C     GM= EULER CONSTANT
      Z=0.0
C     Z= HEIGHT ABOVE GROUND LEVEL
      J=1
      L=100
      M=300
      I=L-1
      P(I)=0.0
      MM=1
C     DO LOOP CALCULATES CONCENTRATION LEVEL AT DISTANCES
C     FROM SOURCE X=20 TO 100 FT
   30 DO 15 K=1,50
      X(K)=K*20
      DO 10 N=100,300
      T=FLOAT(N)/10.
C     T=TIME AFTER RELEASE.  IN THIS CASE 20 SECOND RELEASE
C     IS DIVIDED INTO 200 SMALL PUFFS RELEASED ONE AFTER THE
C     OTHER CONTINUOUSLY.  CONCENTRATIONS AT ALL POINTS IN
C     SPACE DUE TO EACH PUFF WERE OBTAINED USING EQUATION
C     (4.4).  THEY ARE SUPER IMPOSED (ADDED) TO GET THE
C     EXPOSURE DUE TO THE FINITE RELEASE SOURCE.
      G=-1.
      D=B*USTAR*T
C     D= VERTICAL STANDARD DEVIATION
```

APPENDIX II - (Continued)

QUASICONTINUOUS LINE SOURCE

```
      ETA=Z/D
C     ETA= VERTICAL SIMILARITY COORDINATE.
C     HERE E(I) IS OBTAINED FOR INTERMEDIATE VALUES OF ETA
C     BY LINEAR INTERPOLATION WHEN ETA LIES IN BETWEEN DATA
C     POINTS.
      NN=ETA*1000.
      IF(J.EQ.1)GO TO 13
      ER=FLOAT(NN)/1000.
      ERR=ETA-ER
      IF(NN.LE.2000)GO TO 16
      NNN=NN-2000
      LN=NNN/100
      NN=LN+2000
      AAA=NNN
      ER=LN*100
      ERR=(AAA-ER)/1000.
      EI=E(NN)+(E(NN+1)-E(NN))*ERR/0.1
      GO TO 55
   16 AA=NN
      EI=E(NN)+(E(NN+1)-E(NN))*ERR/0.001
   55 G=ALOG(ETA)+GM-1.+EI*EXP(ETA)
   13 R=A*USTAR*T
      XE=X(K)/R-(ALOG(D/Z0)-GM-1.+G)/(A*C)
      F=0.2*(1.-(XE*(XE*XE-3.))/6.)*EXP(-(XE*XE/2.+Z/D))/(2.5*R*D)
C     F=CONTRIBUTION FROM EACH PUFF RELEASED AT A SPACIAL
C     POINT AT A GIVEN TIME.
      IF(F.LT.0.0) F=0.0
   10 P(N)=P(N-1)+F
      Q(K)=P(N-1)
   15 CONTINUE
      MM=MM+1
      IF(MM.EQ.2) GO TO 100
      GO TO 200
C     REST OF THE PROGRAM DOES THE PLOTTING CONCENTRATION
C     FIELD ON A MICRO FILM.
  100 CALL FRAME
      CALL SET(0.1,1.0,0.1,0.9,0.0,2000.,0.0,4.E-3,0,1)
      CALL SETLINE(0)
      CALL GRIDL(10,2,8,5)
      CALL PWRT(288,1024,31H    20SEC.RELEASE-LINE SOURCE    ,31,2,0)
      CALL PWRT(321,1,31H    DISTANCE FROM SOURCE(FT)      ,31,1,0)
      CALL PWRT(1,321,31H CONCENTRATION.(PPM/1,000,000) ,31,1,1)
      CALL CURVE(X,Q,50)
      GO TO 400
```

APPENDIX II - (Continued)

QUASICONTINUOUS LINE SOURCE

```
200 CALL CURVE(X,Q,50)
400 CONTINUE
    IF(Z.GT.3.)GO TO 500
    Z=Z+2.
    J=J+1
    IF(Z.LT.4.5.)GO TO 30
500 Z=Z+4.
    IF(Z.LT.38.5)GO TO 30
    CALL FRAME
    END
```

FIGURES

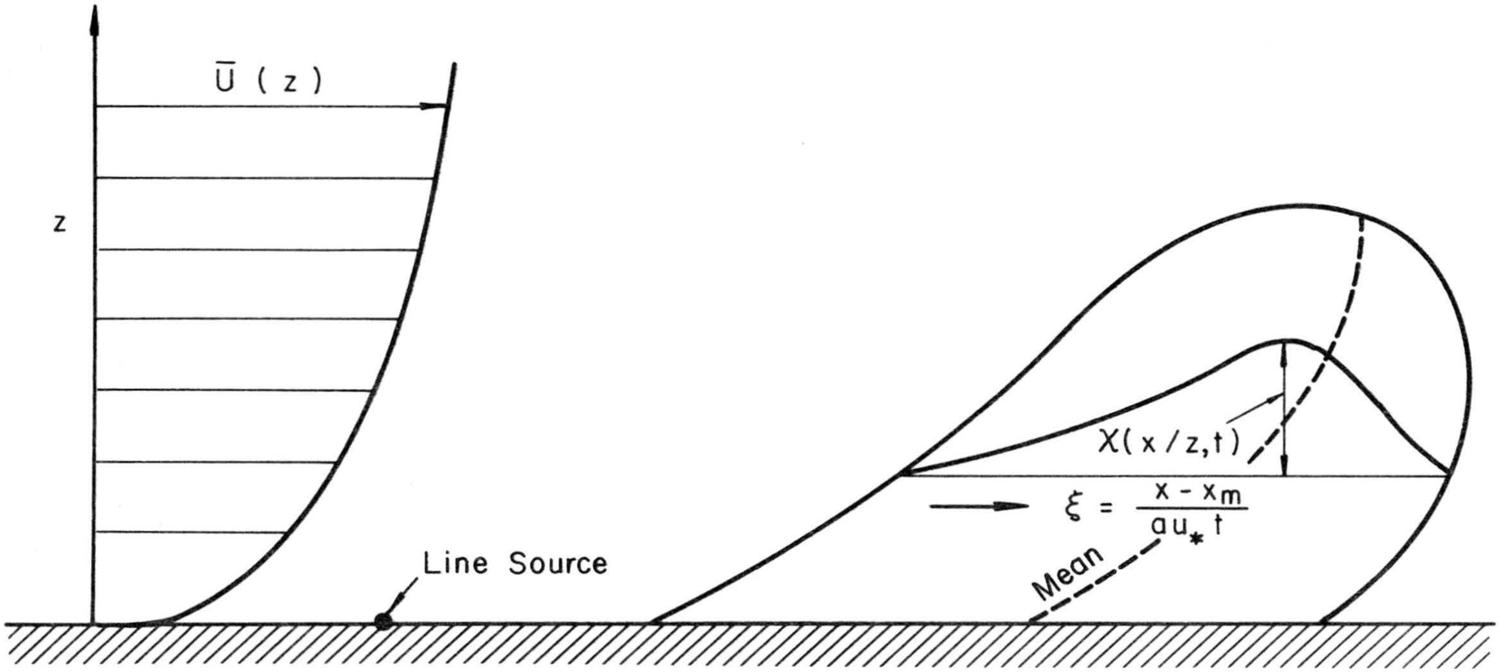

Fig. 1 Cross Section of Dispersing Cloud of Material Released from Instanteneous Line Source Schematic Diagram

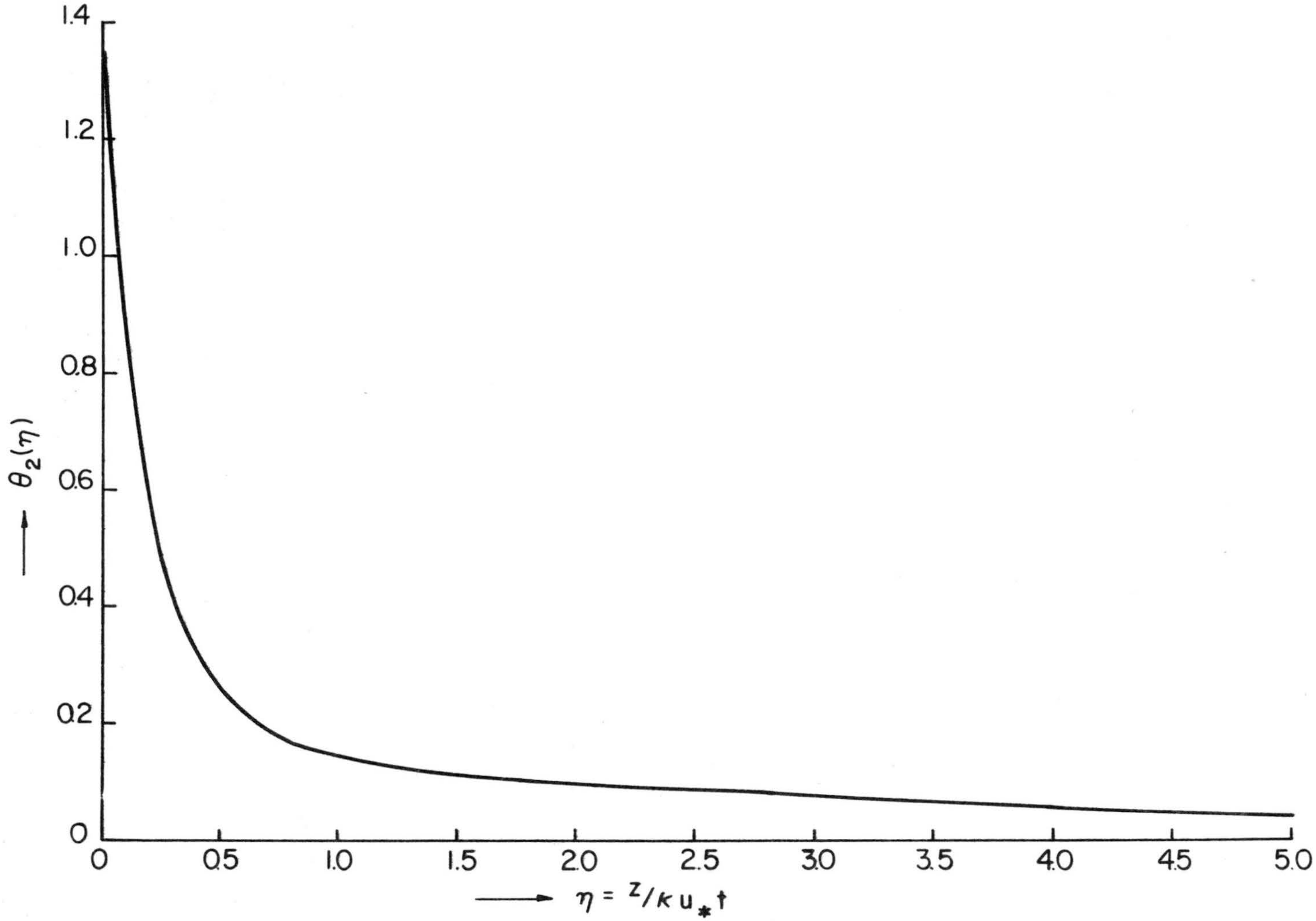

Fig. 2 Second Moment of Longitudinal Density Function

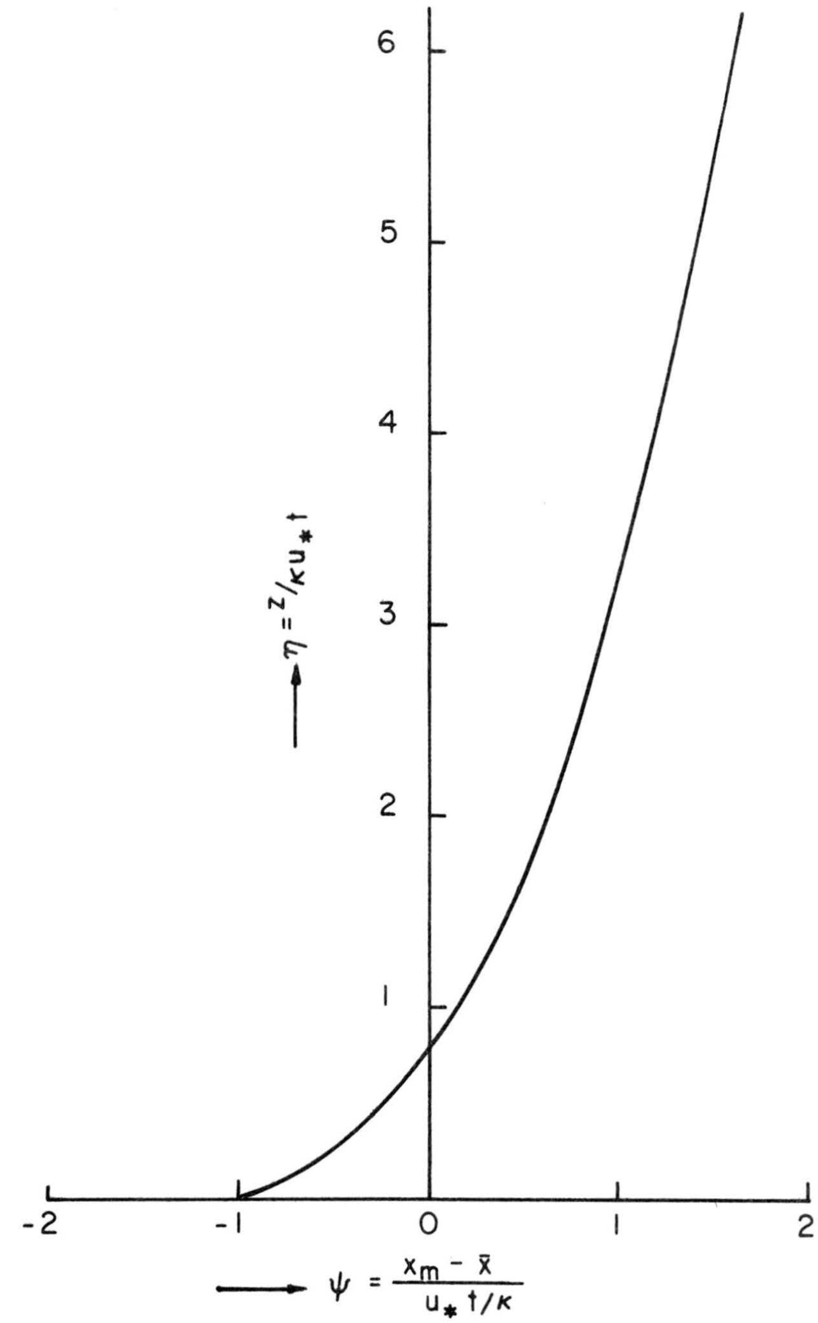

Fig. 3 Mean of Longitudinal Density Function

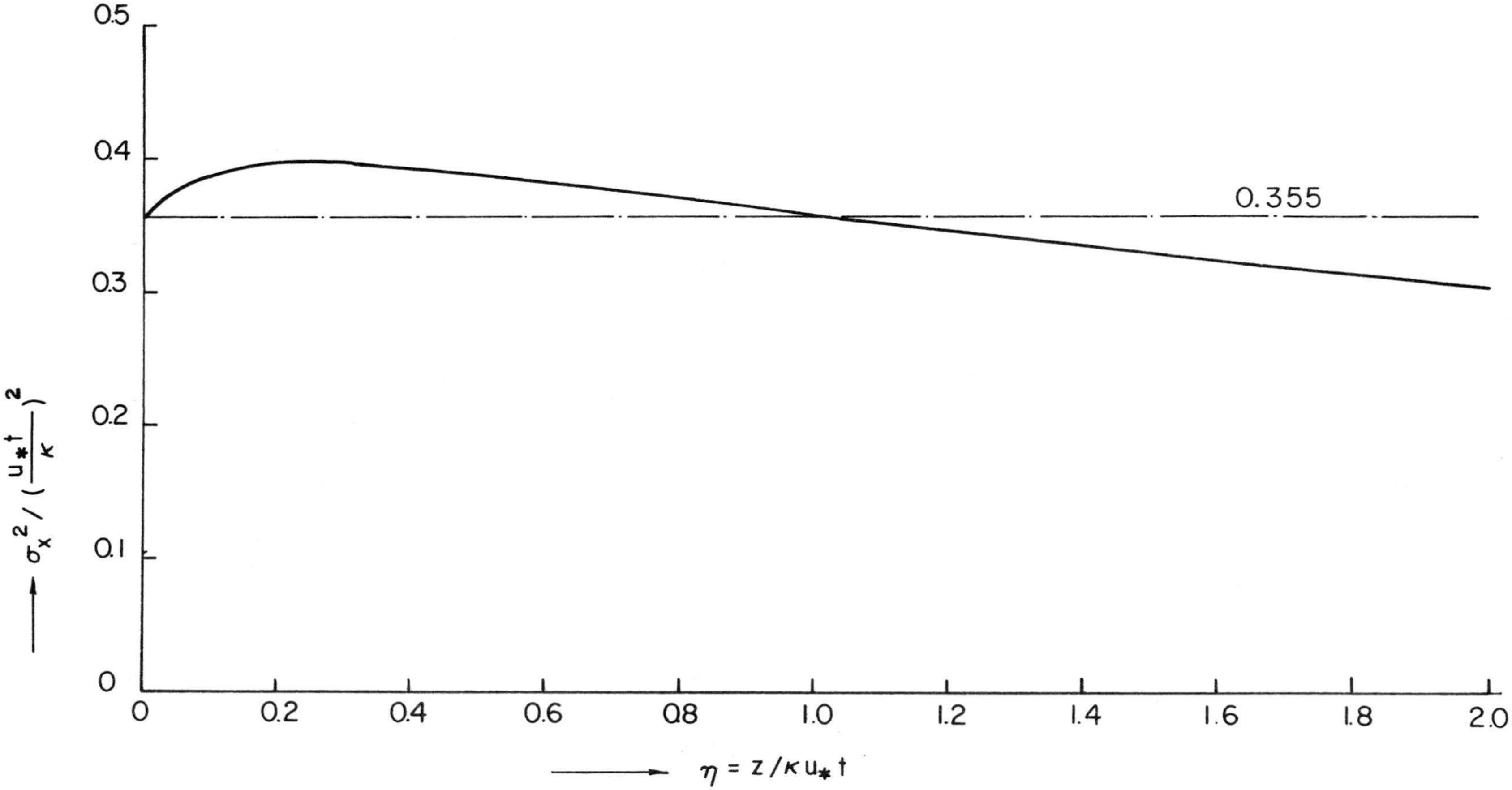

Fig. 4 Variance of Longitudinal Density Function

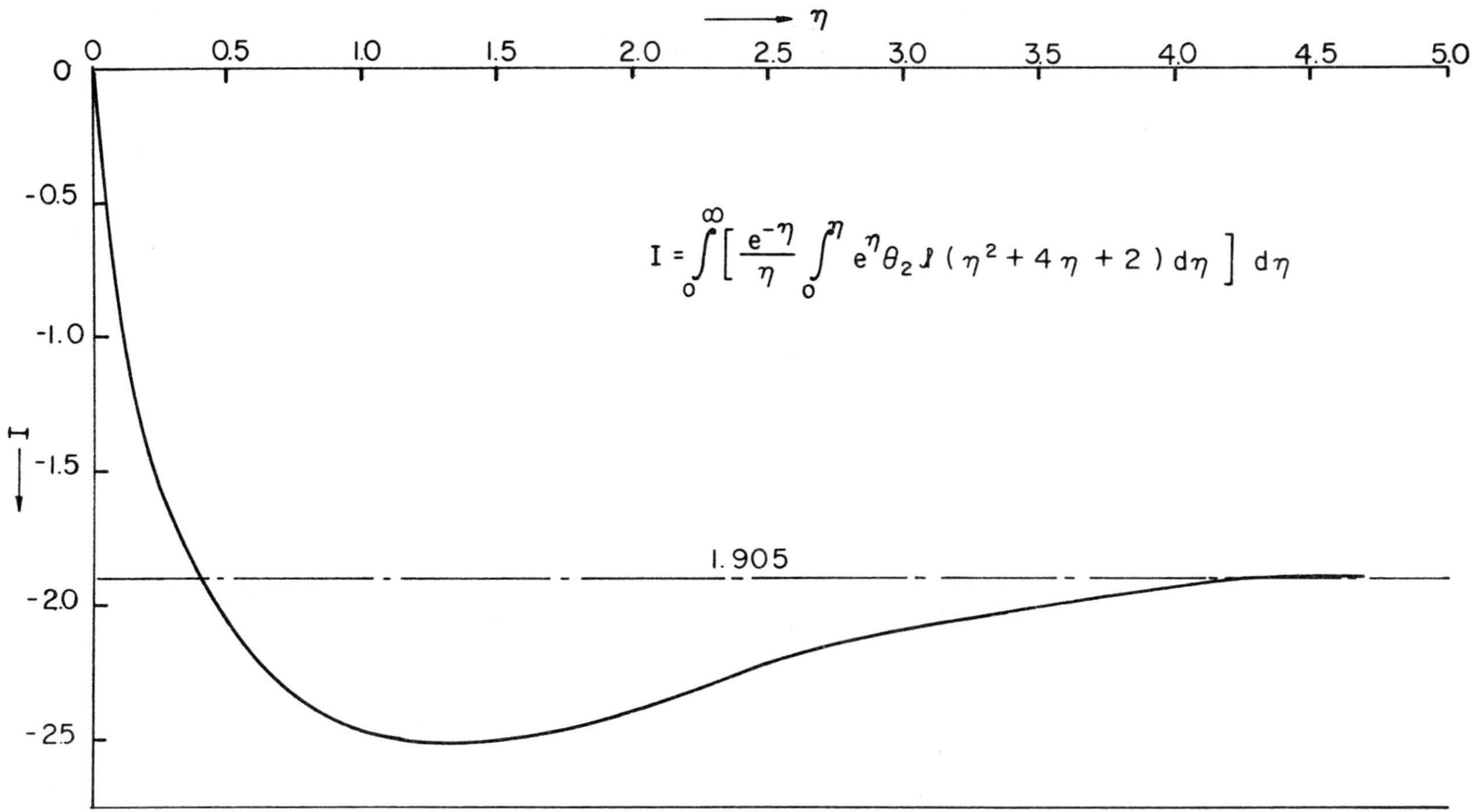

Fig. 5 Integral I

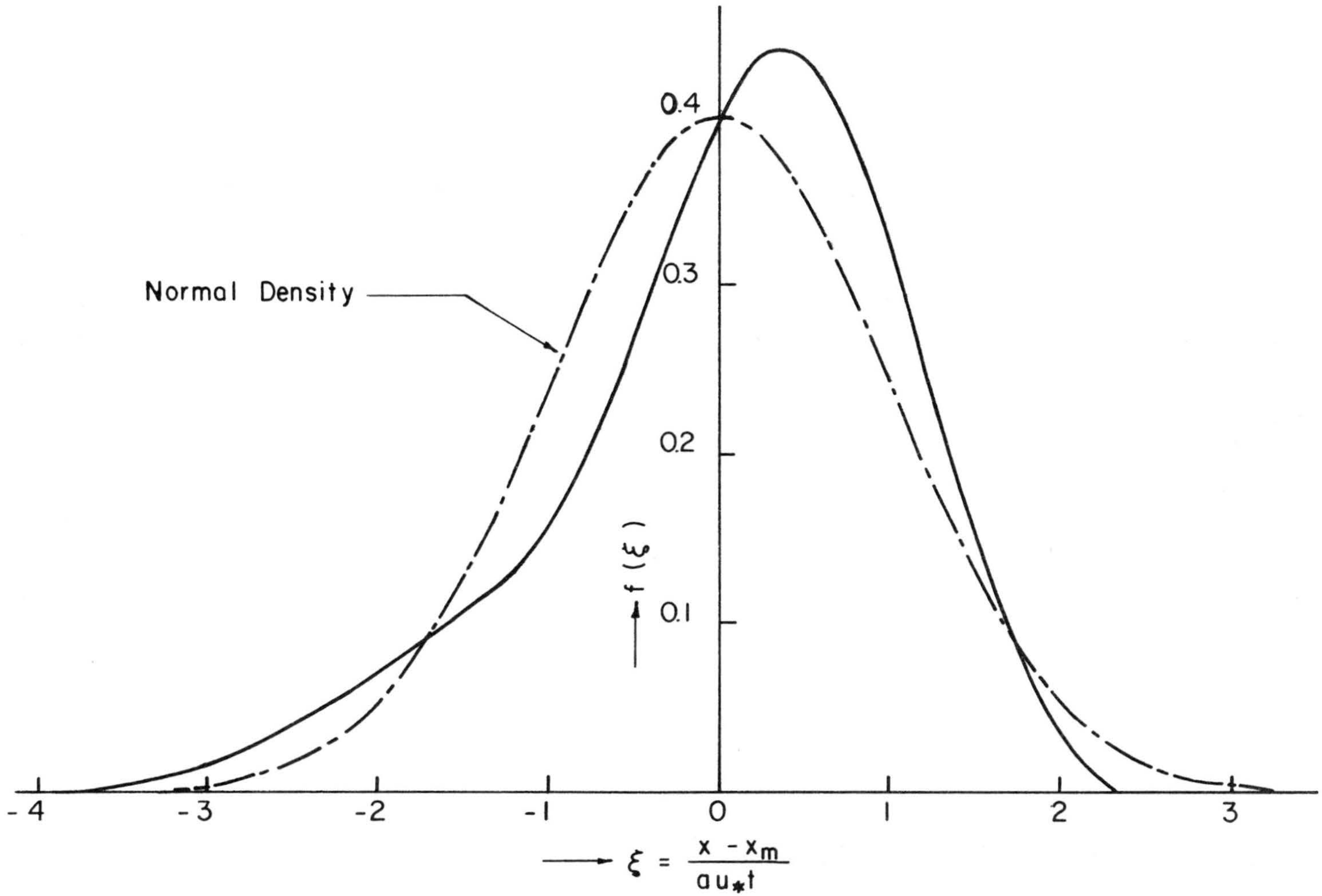

Fig. 6 Density Function for the Direction of Mean Flow

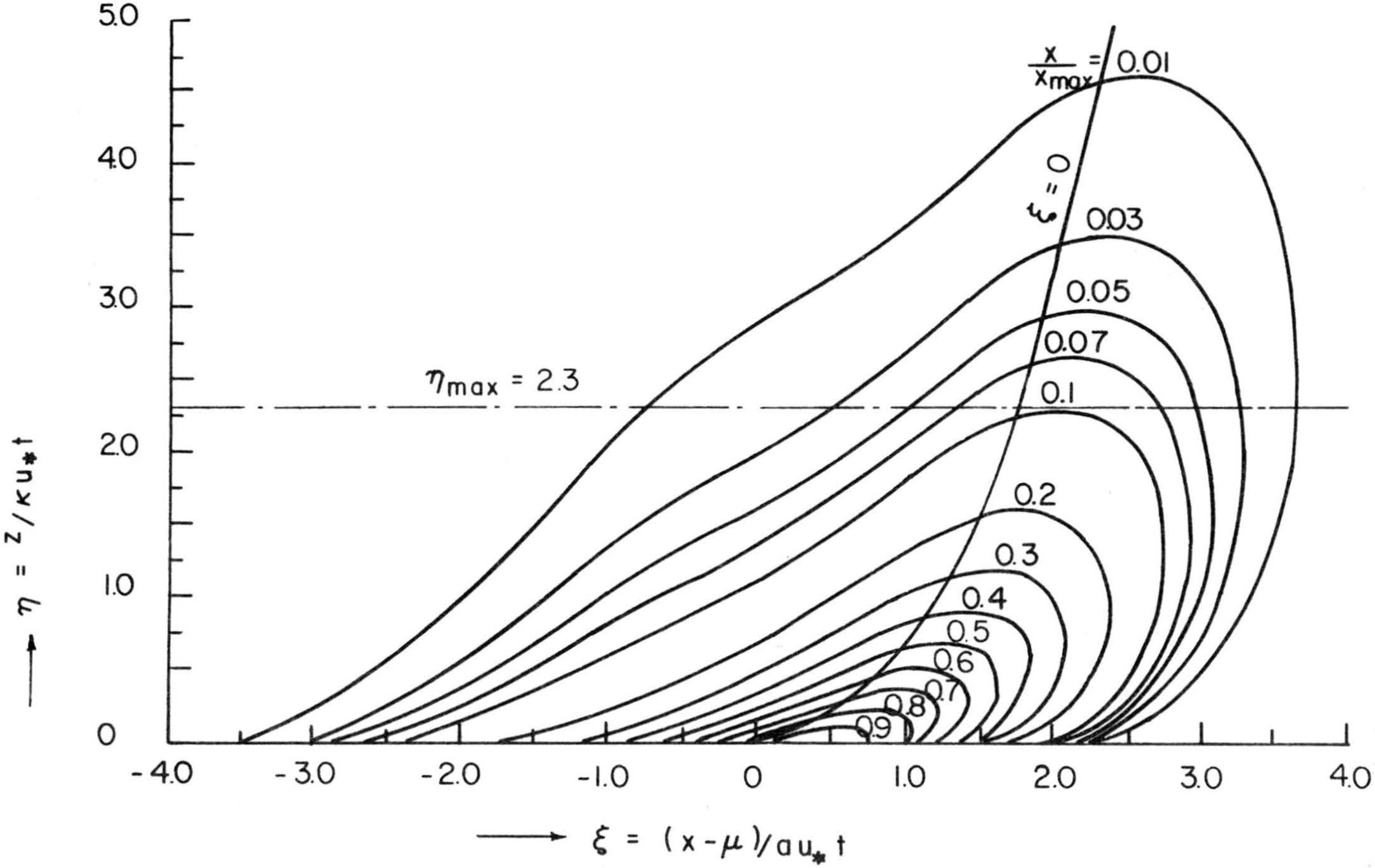

Fig. 7 Shape of Instantaneous Line Source Cloud

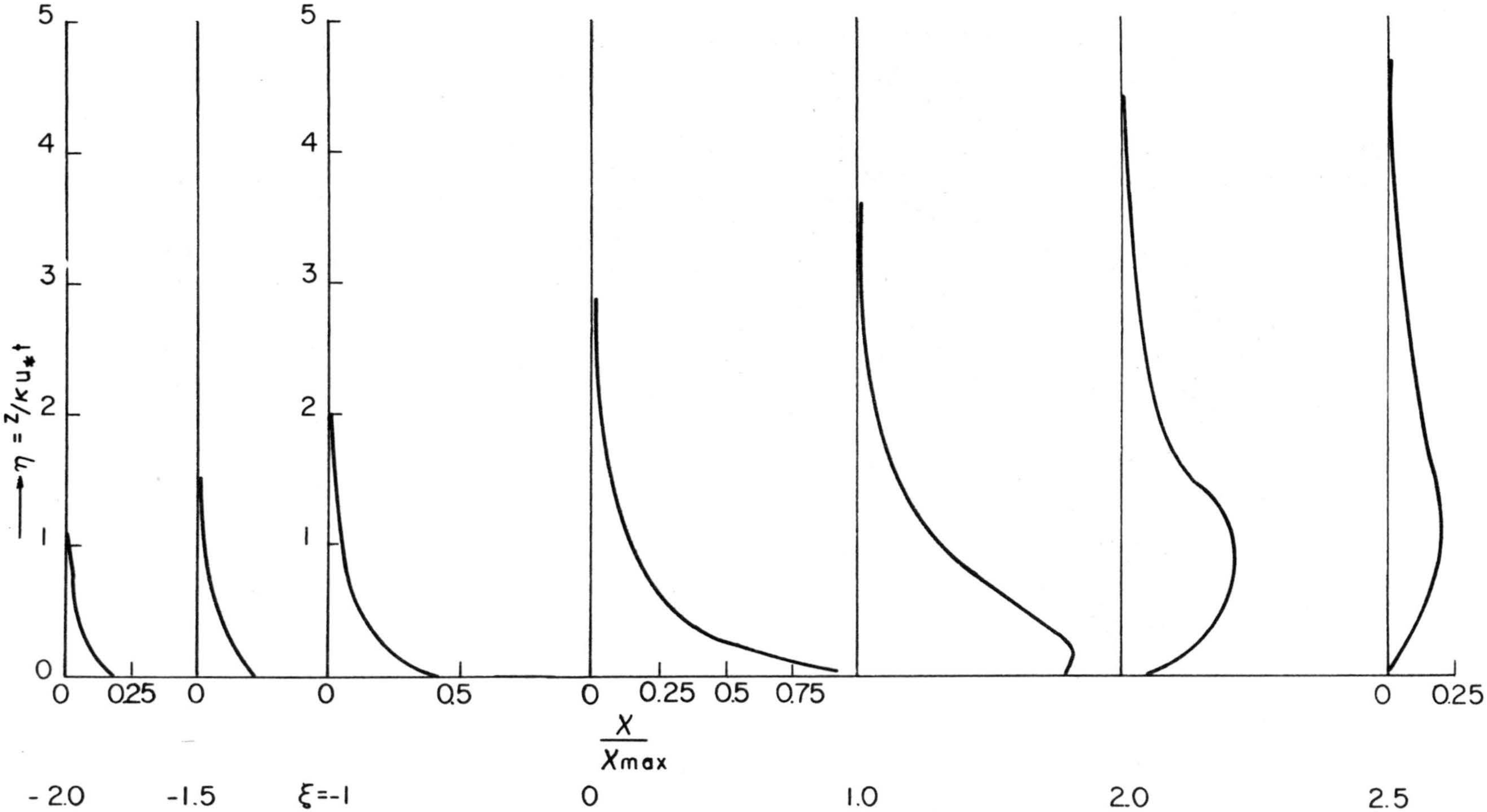

Fig. 8 Vertical Concentration Profiles Within a Smoke Puff

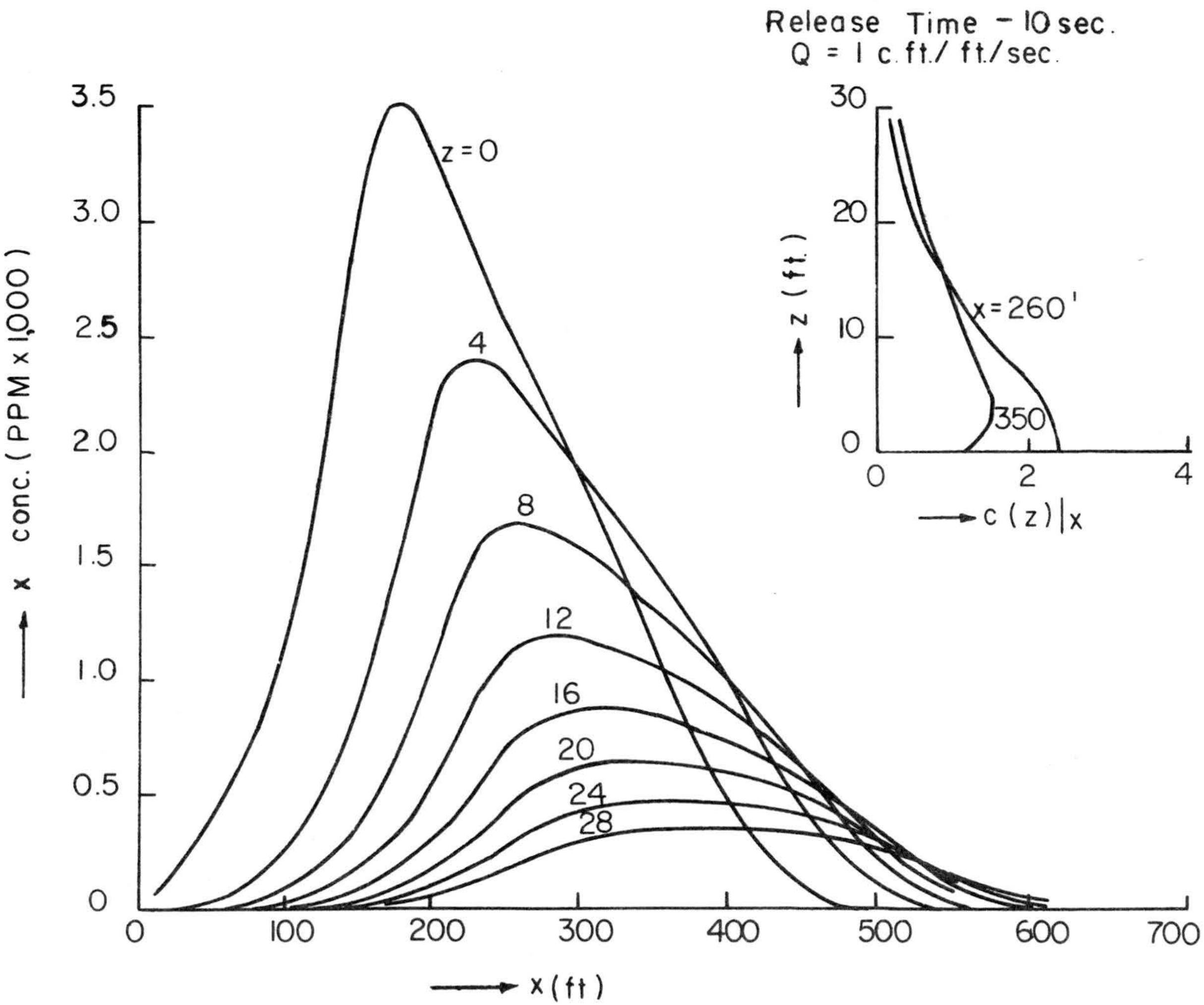

Fig. 9. Quasi Continuous Source

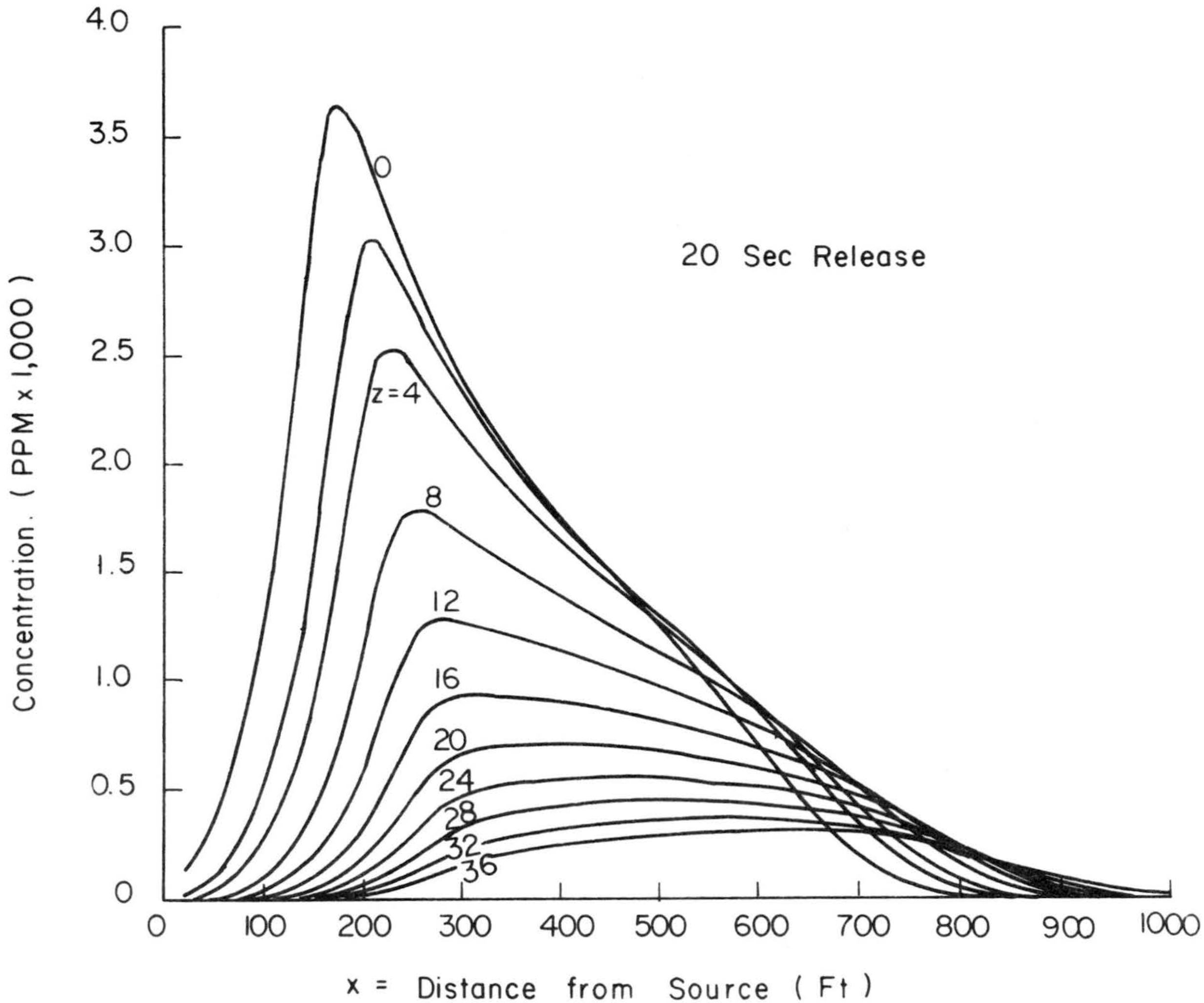

Fig. 10. Quasi Continuous Source

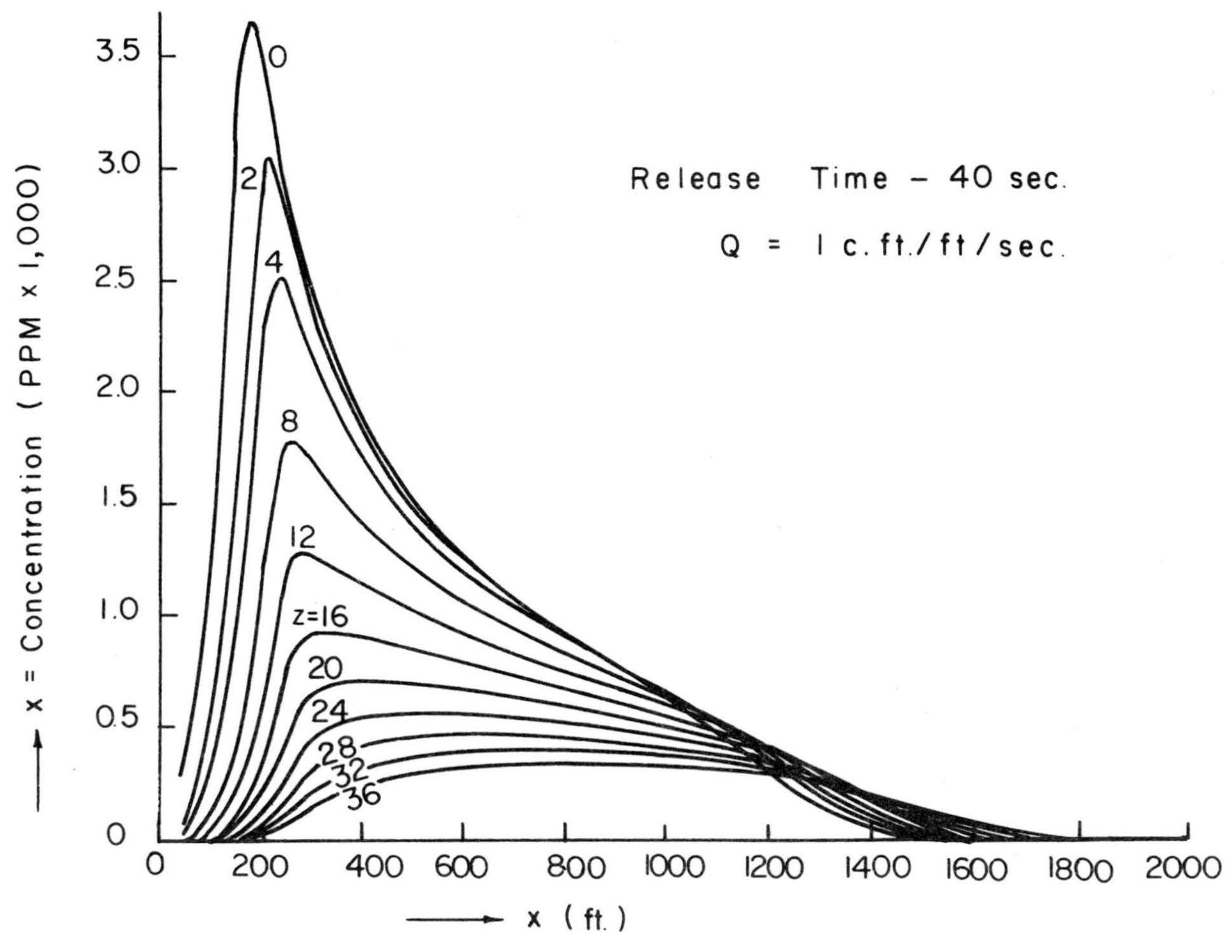

Fig. 11 . Quasi Continuous Source

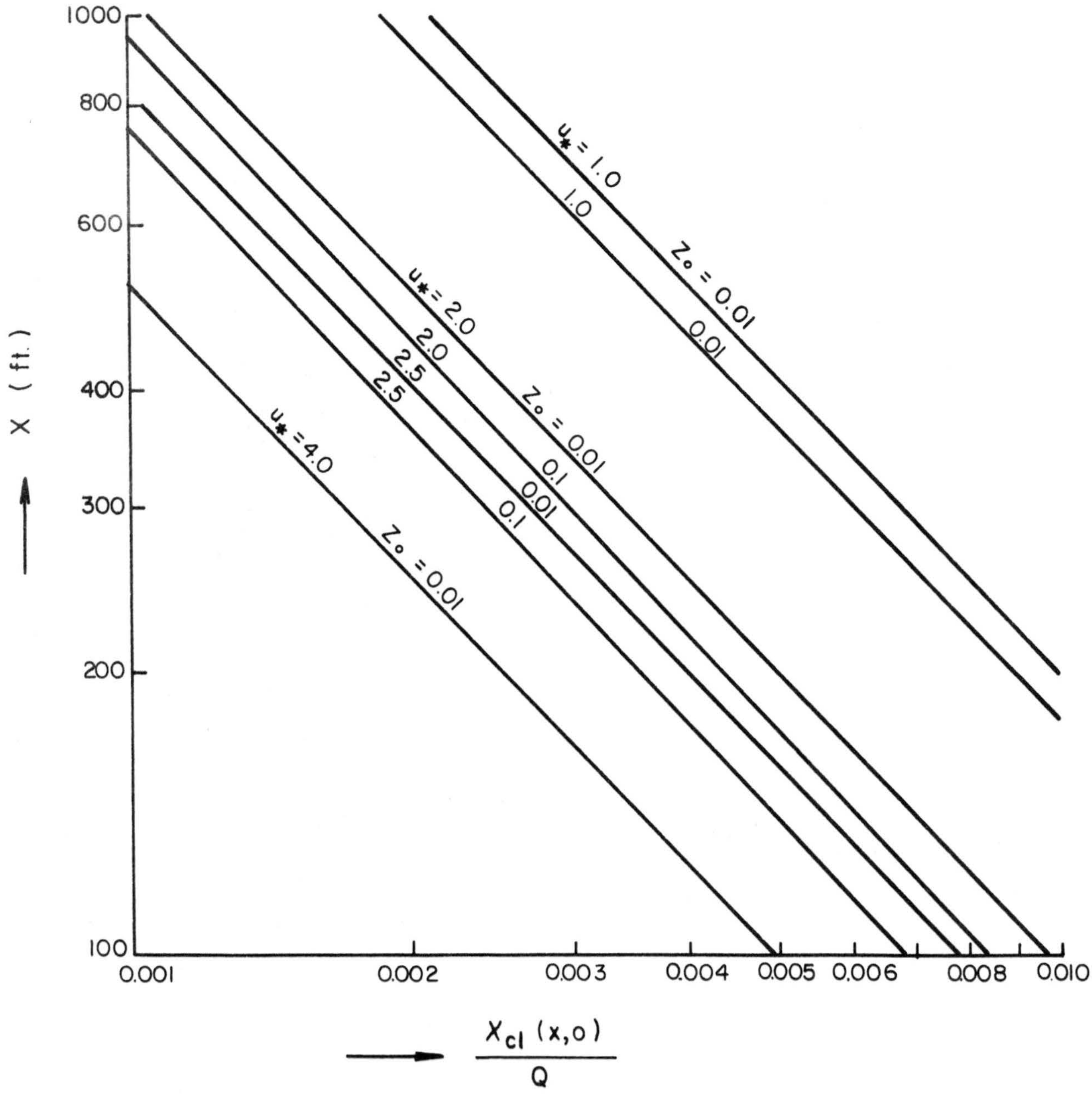

Fig. 12. Effect of u_* and z_o on Continuous Line Source Dispersion Ground Level Concentrations

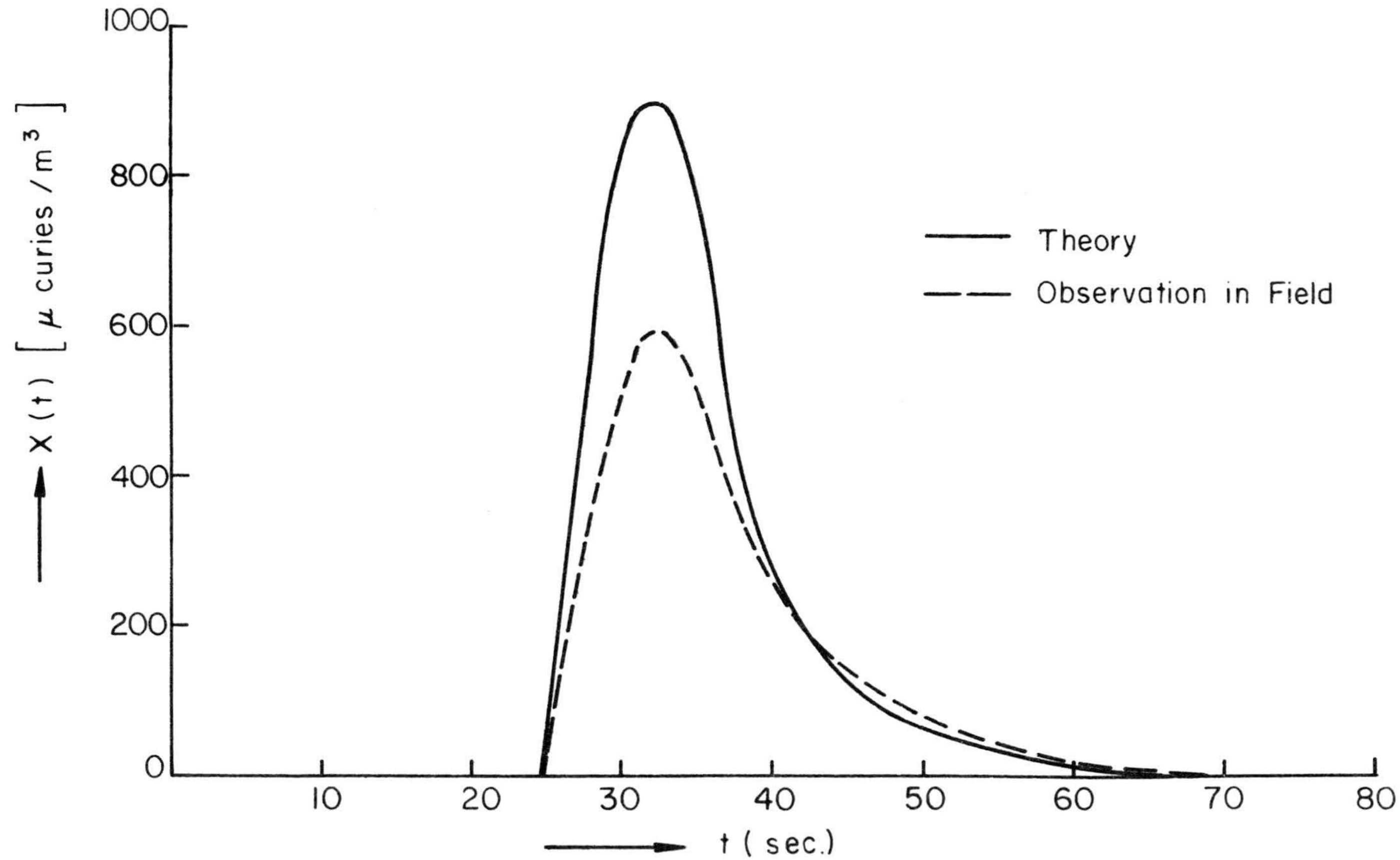

Fig. 13 Exposure at x = 200 m from an Instantaneous Line Source

Theory and Observation

Unclassified
Security Classification

DOCUMENT CONTROL DATA - R & D

(Security classification of title, body of abstract and indexing annotation must be entered when the overall report is classified)

1. ORIGINATING ACTIVITY (Corporate author) Colorado State University Fort Collins, Colorado 80521	2a. REPORT SECURITY CLASSIFICATION 2b. GROUP

3. REPORT TITLE

MASS DISPERSION FROM INSTANTANEOUS LINE SOURCE IN A TURBULENT SHEAR FLOW

4. DESCRIPTIVE NOTES (Type of report and inclusive dates)

Technical report

5. AUTHOR(S) (First name, middle initial, last name)

Putta, Surya Narayana & Cermak, Jack E.

6. REPORT DATE	7a. TOTAL NO. OF PAGES	7b. NO. OF REFS
June 1971	91	29

8a. CONTRACT OR GRANT NO. DAAB07-68-C-0423 and N00014-68-A-0493-0001	9a. ORIGINATOR'S REPORT NUMBER(S) CER71-72SNP-JEC1
b. PROJECT NO. c. d.	9b. OTHER REPORT NO(S) (Any other numbers that may be assigned this report)

10. DISTRIBUTION STATEMENT

Distribution of this document is unlimited

11. SUPPLEMENTARY NOTES	12. SPONSORING MILITARY ACTIVITY
	U. S. Army Material Command Washington D.C.

13. ABSTRACT

Dispersion of passive material released from an instantaneous line source in the constant stress region of a neutral atmosphere is investigated. Concentration fields within the cloud of dispersing material is represented by a three dimensional density function. This density function is divided into a marginal density function and a conditional longitudinal density function. The marginal density function gives the vertical spread of the material. This function has been derived from the semi-empirical equation of dispersion, by using logarithmic velocity distribution for mean velocity and a linear variation for eddy diffusivity in the vertical direction. Longitudinal density function, which gives the longitudinal distribution of material within a given horizontal layer of the cloud, is constructed from the statistical properties of dispersion. Utilizing the Lagrangian similarity hypothesis for the concentration field, the semiempirical equation has been transformed into a similarity coordinate plane. Moment equations are derived from this equation using suitable boundary conditions. From these equations statistical properties are derived for mean, variance and skewness coefficients of the longitudinal density function. It is shown that the longitudinal density function can be well represented by the Gram-Charlier density simply by substituting the derived statistical properties. Ground level concentrations obtained by integration of this proposed density function agree qualitatively with observations in wind tunnels and field experiments.

DD FORM 1 NOV 65 1473

Unclassified
Security Classification

14. KEY WORDS	LINK A		LINK B		LINK C	
	ROLE	WT	ROLE	WT	ROLE	WT
Atmospheric surface layer						
Dispersion						
Instantaneous line source						
Turbulent shear flow						
Statistical properties						
Diffusion						
Air Pollution						

April 1971

DISTRIBUTION LIST FOR UNCLASSIFIED
TECHNICAL REPORTS ISSUED UNDER
CONTRACT N00014-68-A TASK 000-414
0493-0001

Defense Documentation Center
Cameron Station
Alexandria, Virginia 22314 (12)

Technical Library
Naval Ship Research and Development Laboratory
Annapolis, Maryland 21402

Professor Bruce Johnson
Engineering Department
Naval Academy
Annapolis, Maryland 21402

Library
Naval Academy
Annapolis, Maryland 21402

Professor W.R. Debler
Department of Engineering Mechanics
University of Michigan
Ann Arbor, Michigan 48108

Professor W.P. Graebel
Department of Engineering Mechanics
University of Michigan
College of Engineering
Ann Arbor, Michigan 48108

Professor Finn C. Michelsen
Naval Architecture and Marine Engineering
445 West Engineering Building
University of Michigan
Ann Arbor, Michigan 48108

Dr. Francis Ogilvie
Department of Naval Architecture and Marine Engineering
University of Michigan
Ann Arbor, Michigan 48108

Professor W.W. Willmarth
Department of Aerospace Engineering
University of Michigan
Ann Arbor, Michigan 48108

Dr. S.A. Piacsek
Argonne National Laboratory
Applied Mathematics Division
9700 S. Cass Avenue
Argonne, Illinois 60439

AFOSR (REM)
1400 Wilson Boulevard
Arlington, Virginia 22204

Professor S. Corrsin
Mechanics Department
The Johns Hopkins University
Baltimore, Maryland 20910

Professor L.S.G. Kovasznay
The Johns Hopkins University
Baltimore, Maryland 20910

Professor O.M. Phillips
The Johns Hopkins University
Baltimore, Maryland 20910

Librarian
Department of Naval Architecture
University of California
Berkeley, California 94720

Professor Israel Cornet
Department of Mechanical Engineering
University of California
Berkeley, California 94720

Professor M. Holt
Division of Aeronautical Sciences
University of California
Berkeley, California 94720

Professor E.V. Laitone
Department of Mechanical Engineering
University of California
Berkeley, California 94720

Professor P. Lieber
Department of Mechanical Engineering
University of California
Institute of Engineering Research
Berkeley, California 94720

Professor J.R. Paulling
Department of Naval Architecture
University of California
Berkeley, California 94720

Professor J.V. Wehausen
Department of Naval Architecture
University of California
Berkeley, California 94720

Professor E.R. van Driest
Virginia Polytechnic Institute and University
Department of Aerospace Engineering
Blacksburg, Virginia 24061

Commander
Boston Naval Shipyard
Boston, Massachusetts 02129

Director
Office of Naval Research Branch Office
495 Summer Street
Boston, Massachusetts 02210

Commander
Puget Sound Naval Shipyard
Bremerton, Washington 98314

Professor J.J. Foody
Chairman, Engineering Department
State University of New York
Maritime College
Bronx, New York 10465

Dr. Alfred Ritter
Assistant Head, Applied Mechanics Department
Cornell Aeronautical Laboratory, Inc.
Buffalo, New York 14221

Dr. J.W. Morris
Manager, Material Sciences Section
Advanced Materials Research
Bell Aerospace Company
P.O. Box 1
Buffalo, New York 14240

Professor G.H. Carrier
Department of Engineering and Applied Physics
Harvard University
Cambridge, Massachusetts 02138

Commanding Officer
NROTC Naval Administrative Unit
Massachusetts Institute of Technology
Cambridge, Massachusetts 02139

Professor M.A. Abkowitz
Department of Naval Architecture and Marine Engineering
Massachusetts Institute of Technology
Cambridge, Massachusetts 02139

Professor A.T. Ippen
Department of Civil Engineering
Massachusetts Institute of Technology
Cambridge, Massachusetts 02139

Professor L.N. Howard
Department of Mathematics
Massachusetts Institute of Technology
Cambridge, Massachusetts 02139

Professor E.W. Merrill
Department of Mathematics
Massachusetts Institute of Technology
Cambridge, Massachusetts 02139

Professor E. Mollo-Christensen
Room 54-1722
Massachusetts Institute of Technology
Cambridge, Massachusetts 02139

Professor N. Newman
Department of Naval Architecture and Marine Engineering
Massachusetts Institute of Technology
Cambridge, Massachusetts 02139

Professor A.H. Shapiro
Department of Mechanical Engineering
Massachusetts Institute of Technology
Cambridge, Massachusetts 02139

Commander
Charleston Naval Shipyard
U.S. Naval Base
Charleston, South Carolina 29408

A.R. Kuhlthau, Director
Research Laboratories for the Engineering Sciences
Thorton Hall, University of Virginia
Charlottesville, Virginia 22903

Director
Office of Naval Research Branch Office
536 South Clark Street
Chicago, Illinois 60605

Library
Naval Weapons Center
China Lake, California 93555

Professor J.M. Burgers
Institute of Fluid Dynamics and Applied Mathematics
University of Maryland
College Park, Maryland 20742

Professor Pai
Institute for Fluid Dynamics and Applied Mathematics
University of Maryland
College Park, Maryland 20740

Acquisition Director
NASA Scientific & Technical Information
P.O. Box 33
College Park, Maryland 20740

Technical Library
Naval Weapons Laboratory
Dahlgren, Virginia 22448

Computation & Analyses Laboratory
Naval Weapons Laboratory
Dahlgren, Virginia 22448

Dr. C.S. Wells, Jr.
Manager - Fluid Mechanics
Advanced Technology Center, Inc.
P.O. Box 6144
Dallas, Texas 75222

Dr. R.H. Kraichnan
Dublin, New Hampshire 03444

Commanding Officer
Army Research Office
Box CM, Duke Station
Durham, North Carolina 27706

Professor A. Charnes
The Technological Institute
Northwestern University
Evanston, Illinois 60201

Dr. Martin H. Bloom
Polytechnic Institute of Brooklyn
Graduate Center, Dept. of Aerospace
Engineering and Applied Mechanics
Farmingdale, New York 11735

Technical Documents Center
Building 315
U.S. Army Mobility Equipment
Research and Development Center
Fort Belvoir, Virginia 22060

Professor J.E. Cermak
College of Engineering
Colorado State University
Ft. Collins, Colorado 80521

Technical Library
Webb Institute of Naval Architecture
Glen Cove, Long Island, New York 11542

Professor E.V. Lewis
Webb Institute of Naval Architecture
Glen Cove, Long Island, New York 11542

Dr. B.N. Pridmore Brown
Northrop Corporation
NORAIR-Div.
Hawthorne, California 90250

Dr. J.P. Breslin
Stevens Institute of Technology
Davidson Laboratory
Hoboken, New Jersey 07030

Dr. D. Savitsky
Stevens Institute of Technology
Davidson Laboratory
Hoboken, New Jersey 07030

Mr. C.H. Henry
Stevens Institute of Technology
Davidson Laboratory
Hoboken, New Jersey 07030

Dr. J.P. Craven
University of Hawaii
1801 University Avenue
Honolulu, Hawaii 96822

Professor E.L. Resler
Graduate School of Aeronautical Engineering
Cornell University
Ithaca, New York 14851

Professor John Miles
c/o I.G.P.P.
University of California, San Diego
La Jolla, California 92038

Director
Scrippe Institution of Oceanography
University of California
La Jolla, California 92037

Professor A. Ellis
University of California, San Diego
Department of Aerospace & Mechanical Engineering
La Jolla, California 92037

Dr. B. Sternlicht
Mechanical Technology Incorporated
968 Albany-Shaker Road
Latham, New York 12110

Dr. Coda Pan
Mechanical Technology Incorporated
968 Albany-Shaker Road
Latham, New York 12110

Mr. P. Eisenberg, President
Hydronautics, Inc.
Pindell School Road
Howard County
Laurel, Maryland 20810

Mr. M.P. Tulin
Hydronautics, Inc.
Pindell School Road
Howard County
Laurel, Maryland 20810

Mr. Alfonso Alcedan L.,Director
Laboratorio Nacional De Hydraulics
Antigui Cameno A. Ancon
Casilla Jostal 682
Lima, Peru

Commander
Long Beach Naval Shipyard
Long Beach, California 90802

Professor John Laufer
Department of Aerospace Engineering
University Park
Los Angeles, California 9000⁷

Professor J.M. Killen
St. Anthony Falls Hydraulic Lab.
University of Minnesota
Minneapolis, Minnesota 55414

Lorenz G. Straub Library
St. Anthony Falls Hydraulic Lab.
Mississippi River at 3rd Avenue S.E.
Minneapolis, Minnesota 55414

Professor J. Ripkin
St. Anthony Falls Hydraulic Lab.
University of Minnesota
Minneapolis, Minnesota 55414

Dr. W. Silberman
St. Anthony Falls Hydraulic Lab.
Mississippi River at 3rd Avenue S.E.
Minneapolis, Minnesota 55414

Superintendent
Naval Postgraduate School
Library Code 0212
Monterey, California 93940

Professor A.B. Metzner
University of Delaware
Newark, New Jersey 19711

Technical Library
Naval Underwater Systems Center
Newport, Rhode Island 02840

Professor Dudley D. Fuller
Department of Mechanical Engineering
Columbia University
New York, New York 10027

Professor V. Castelli
Department of Mechanical Engineering
Columbia University
New York, New York 10027

Professor H. Elrod
Department of Mechanical Engineering
Columbia University
New York, New York 10027

Professor J.J. Stoker
Institute of Mathematical Sciences
New York University
251 Mercer Street
New York, New York 10003

Society of Naval Architects and Marine Engineering
74 Trinity Place
New York, New York 10006

Engineering Societies Library
345 East 47th Street
New York, New York 10017

Office of Naval Research
New York Area Office
207 W. 24th Street
New York, New York 10011

Miss O.M. Leach, Librarian
National Research Council
Aeronautical Library
Montreal Road
Ottawa 7, Canada

Technical Library
Naval Ship Research and Development Center
Panama City, Florida 32401

Technical Library
Naval Undersea R & D Center
Pasadena Laboratory
3202 E. Foothill Boulevard
Pasadena, California 91107

Dr. Andrew Fabula
Naval Undersea Research & Development Center
Pasadena Laboratory
3202 E. Foothill Boulevard
Pasadena, California 91107

Dr. J.W. Hoyt
Naval Undersea R & D Center
Pasadena Laboratory
3202 E. Foothill Boulevard
Pasadena, California 91107

Professor A. Acosta
Department of Mechanical Engineering
California Institute of Technology
Pasadena, California 91109

Professor H. Liepmann
Department of Aeronautics
California Institute of Technology
Pasadena, California 91109

Professor M.S. Plesset
Engineering Division
California Institute of Technology
Pasadena, California 91109

Professor A. Roshko
California Institute of Technology
Pasadena, California 91109

Professor T.Y. Wu
Department of Engineering
California Institute of Technology
Pasadena, California 91109

Director
Office of Naval Research Branch Office
1030 E. Green Street
Pasadena, California 91101

Naval Ship Engineering Center
Philadelphia Division
Technical Library
Philadelphia, Pennsylvania 19112

Technical Library
Philadelphia Naval Shipyard
Philadelphia, Pennsylvania 19112

Professor R.C. Mac Camy
Department of Mathematics
Carnegie Institute of Technology
Pittsburgh, Pennsylvania 15213

Dr. Paul Kaplan
Oceanics, Inc.
Plainview, Long Island, New York 11803

Technical Library
Naval Missile Center
Point Mugu, California 93441

Technical Library
Naval Civil Engineering Laboratory
Port Hueneme, California 93041

Commander
Portsmouth Naval Shipyard
Portsmouth, New Hampshire 03801

Commander
Norfolk Naval Shipyard
Portsmouth, Virginia 23709

Professor F.E. Bisshopp
Division of Engineering
Brown University
Providence, Rhode Island 02912

Dr. William A. Gross, Vice President
Ampex Corporation
401 Broadway
Redwood City, California 94063

Dr. H.N. Abramson
Southwest Research Institute
8500 Culebra Road
San Antonio, Texas 78228

Editor
Applied Mechanics Review
Southwest Research Institute
8500 Culebra Road
San Antonio, Texas 78206

Office of Naval Research
San Francisco Area Office
50 Fell Street
San Francisco, California 94102

Library
Pearl Harbor Naval Shipyard
Box 400
FPO San Francisco, California 96610

Technical Library
Hunters Point Naval Shipyard
San Francisco, California 94135

Librarian
Naval Ordnance Laboratory
White Oak
Silver Spring, Maryland 20910

Fenton Kennedy Document Library
The Johns Hopkins University
Applied Physics Laboratory
8621 Georgia Avenue
Silver Spring, Maryland 20910

Professor E.Y. Hsu
Department of Civil Engineering
Stanford University
Stanford, California 94305

Dr. Byrne Perry
Department of Civil Engineering
Stanford University
Stanford, California 94305

Dr. R.L. Street
Department of Civil Engineering
Stanford University
Stanford, California 94305

Professor Milton Van Dyke
Department of Aeronautical Engineering
Stanford University
Stanford, California 94305

Professor R.C. Di Prima
Department of Mathematics
Rensselaer Polytechnic Institute
Troy, New York 12180

Professor J. Lumley
Ordnance Research Laboratory
Pennsylvania State University
University Park, Pennsylvania 16801

Dr. M. Sevik
Ordnance Research Laboratory
Pennsylvania State University
University Park, Pennsylvania 16801

Dr. J.M. Robertson
Department of Theoretical and Applied Mechanics
University of Illinois
Urbana, Illinois 61803

Technical Library
Mare Island Naval Shipyard
Vallejo, California 94592

Code 438
Office of Naval Research
Department of the Navy
Arlington, Virginia 22217 (3)

Code 461
Office of Naval Research
Department of the Navy
Arlington, Virginia 22217

Code 463
Office of Naval Research
Department of the Navy
Arlington, Virginia 22217

Code 472
Office of Naval Research
Department of the Navy
Arlington, Virginia 22217

Code 468
Office of Naval Research
Department of the Navy
Arlington, Virginia 22217

Code 473
Office of Naval Research
Department of the Navy
Arlington, Virginia 22217

Code 481
Office of Naval Research
Department of the Navy
Arlington, Virginia 22217

Code 2627
Naval Research Laboratory
Washington, D.C. 20390 (6)

Library, Code 2620 (ONRL)
Naval Research Laboratory
Washington, D.C. 20390 (6)

Code 6170
Naval Research Laboratory
Washington, D.C. 20390

Code 4000
Director of Research
Naval Research Laboratory
Washington, D.C. 20390

Code 8030 (Maury Center)
Naval Research Laboratory
Washington, D.C. 20390

Code 8040
Naval Research Laboratory
Washington, D.C. 20390

Code 031
Naval Ship Systems Command
Washington, D.C. 20390

Code 0341
Naval Ship Systems Command
Washington, D.C. 20390

Code 03412B (L. Benen)
Naval Ship Systems Command
Washington, D.C. 20390

Code 03412 (J. Schuler)
Naval Ship Systems Command
Washington, D.C. 20390

Code 2052
Naval Ship Systems Command
Washington, D. C. 20390

Code 6034
Naval Ship Engineering Center
Center Building
Prince George's Center
Hyattsville, Maryland 20782

Code 6110
Naval Ship Engineering Center
Center Building
Prince George's Center
Hyattsville, Maryland 20782

Code 6113
Naval Ship Engineering Center
Center Building
Prince George's Center
Hyattsville, Maryland 20782

Code 6114
Naval Ship Engineering Center
Center Building
Prince George's Center
Hyattsville, Maryland 20782

Code 6120E
Naval Ship Engineering Center
Center Building
Prince George's Center
Hyattsville, Maryland 20782

Code 6136
Naval Ship Engineering Center
Center Building
Prince George's Center
Hyattsville, Maryland 20782

Dr. A. Powell
Code 01
Naval Ship Research and Development Center
Washington, D.C. 20034

Mr. W.M. Ellsworth
Code OH50
Naval Ship Research and Development Center
Washington, D.C. 20034

Central Library
Code L42
Naval Ship Research and Development Center
Washington, D.C. 20034

Dr. W.E. Cummins
Code 500
Naval Ship Research and Development Center
Washington, D.C. 20034

Mr. S.F. Crump
Code 513
Naval Ship Research and Development Center
Washington, D.C. 20034

Mr. R. Wermter
Code 520
Naval Ship Research and Development Center
Washington, D.C. 20034

Dr. P. Pien
Code 521
Naval Ship Research and Development Center
Washington, D.C. 20034

Dr. W.B. Morgan
Code 540
Naval Ship Research and Development Center
Washington, D.C. 20034

Mr. P. Granville
Code 541
Naval Ship Research and Development Center
Washington, D.C. 20034

Mr. J.B. Hadler
Code 560
Naval Ship Research and Development Center
Washington, D.C. 20034

Dr. H.R. Chaplin
Code 600
Naval Ship Research and Development Center
Washington, D.C. 20034

Mr. G.H. Gleissner
Code 800
Naval Ship Research and Development Center
Washington, D.C. 20034

Dr. M. Strasberg
Code 901
Naval Ship Research and Development Center
Washington, D.C. 20034

Mr. J. McCarthy
Code 552
Naval Ship Research and Development Center
Washington, D.C. 20034

Code 03
Naval Air Systems Command
Washington, D.C. 20360

AIR 5301
Naval Air Systems Command
Department of the Navy
Washington, D.C. 20360

Code ORD 03
Naval Ordnance Systems Command
Washington, D.C. 20360

Code ORD 035
Naval Ordnance Systems Command
Washington, D.C. 20360

Code ORD 05413
Naval Ordnance Systems Command
Washington, D.C. 20360

Code ORD 9132
Naval Ordnance Systems Command
Washington, D.C. 20360

Oceanographer of the Navy
Washington, D.C. 20390

Commander
Naval Oceanographic Office
Washington, D.C. 20390

Chief Scientist (CNM PM-1)
Strategic Systems Project Office
Department of the Navy
Washington, D.C. 20360

Technical Division (CNM PM 11-20)
Deep Submergence Systems Project Office
Department of the Navy
Washington, D.C. 20360

Dr. A.L. Slafkosky
Scientific Advisor
Commandant of the Marine Corps (Code AX)
Washington, D.C. 20380

Librarian Station 5-2
Coast Guard Headquarters
NASSIF Building
400 7th Street, S.W.
Washington, D.C. 20591

Office of Research and Development
Maritime Administration
441 G. Street, N.W.
Washington, D.C. 20235

Division of Ship Design
Maritime Administration
441 G. Street, N.W.
Washington, D.C. 20235

National Science Foundation
Engineering Division
1800 G. Street, N.W.
Washington, D.C. 20550

Dr. G. Kulin
National Bureau of Standards
Washington, D.C. 20234

Science & Technology Division
Library of Congress
Washington, D.C. 20540

Chief of Research & Development
Office of Chief of Staff
Department of the Army
The Pentagon, Washington, D.C. 20310

Professor A. Thiruvengadam
Department of Mechanical Engineering
The Catholic University of America
Washington, D.C. 20017

Professor G. Birkhoff
Department of Mathematics
Harvard University
Cambridge, Massachusetts 02138

AIR 604
Naval Air Systems Command
Department of the Navy
Washington, D.C. 20360

Dr. A.S. Iberall, President
General Technical Services, Inc.
451 Penn Street
Yeadon, Pennsylvania 19050

Professor J.F. Kennedy, Director
Iowa Institute of Hydraulic Research
State University of Iowa
Iowa City, Iowa 52240

Professor L. Landweber
Iowa Institute of Hydraulic Research
State University of Iowa
Iowa City, Iowa 52240

Dr. Lee Segel
Department of Mathematics
Rensselaer Polytechnic Institute
Troy, New York 12180

Code 6101E
Naval Ship Engineering Center
Center Building
Prince George's Center
Hyattsville, Maryland 20782